

We thank the two reviewers for their time and effort in the review process. We appreciate their helpful and constructive comments and suggestions, which improve the quality of the paper. We have taken into account all the comments and revised our manuscript accordingly. Please see below for details (Reviewer comments are in blue).

Anonymous Referee #1

General Comments

In the present manuscript the authors analyse whether a globally refined model (RRM) can be used instead of a globally high-resolution model (HRM). The RRM is computationally less demanding than the HRM. The authors compare different atmospheric quantities of simulations with the RRM, the HRM and a coarse grid global model (LRM). The RRM was run in to different configurations. One using the LRM physics and the other the HRM physics. The authors conclude that the RRM is a useful tool for high resolution developments.

The manuscript needs major additions and major revisions (see specific comments below). After taking care of these the manuscript may be published in GMD.

Specific Comments

Comments regarding the GMD principal criteria

Scientific significance - Excellent

I am not aware of any publication that analyses in detail the effect of coarse grid global model, fine grid global model, coarse grid model with regional refined grid and tests of different physics tuning in the regional refinement.

Thanks. We are glad that our study fills this gap in the literature.

Scientific quality - Good

The overall scientific quality is good. A major deficiency is that the cited literature in the manuscript is heavily "American" weighted. The authors should increase their literature study of articles outside of the U.S.. They would have been aware of the remarks under item 4 in "Other specific comments" below.

Thanks for pointing out this limitation. We revised the manuscript to include more non-US references as suggested. See the response to specific comments below for details.

Scientific reproducibility - Poor

The link to the source code of the model is given at the end of the manuscript <https://github.com/E3SM-Project/E3SM>. However, this information is not enough to reproduce the science by a fellow scientist. What at least is missing:

- exact information where to get the observational and reanalysis data from. This can be provided by web links in table 2. Even this may be not enough, therefore comments on what has to be taken into account additionally should be added if needed.

The web links of the observational and reanalysis data used in this study were added in the last column of Table 2. These locations are also documented in the acknowledgement session.

- detailed technical model simulation setup (can be put into the Appendix). Actually, every information that is needed to run the model simulations as the authors did.

We added two new Tables (Tables A1 and A2) in the Appendix for the model simulation setup details, including code hash numbers, grids, configurations, and non-default parameter changes.

- post processing tools used for the statistical analyses

We used the NCL built-in function “ttest” for the Student’s t-test in the paper.

- time period(s) of simulations (see item 3 under "Other specific comments" below.

See answers in item 3 below.

presentation quality - Good

The presentation of the results is overall good in a well-structured way. However, it misses some important information (see "Other specific comments" below)

Other specific comments

1. The authors claim to use a "fully-coupled Earth system model", however, in "2.1 Model overview and experiment design" they describe only the atmospheric part. What about the ocean? What about the coupling?

Sorry for the confusion. The fully-coupled Earth system model (E3SM) shares the same code repository with its atmosphere model (EAM). Therefore, with the same code repository, users have the option to run either the coupled simulation or the atmosphere-only simulation. We only used the atmosphere-only simulations in the present study, and thus only described the atmosphere model.

We added the following clarification on P4 L10, “Since all the simulations analysed here are atmosphere-only ones, we only provide information about the atmosphere model. Details about the coupled E3SM model can be found in Golaz et al. (2019).”.

2. page 5, line 7-8 "The LRM and HRM physics time steps are 30 minutes and 15 minutes, respectively". What about the dynamic time step? The dynamic time step depends on the grid width. How do the authors set the time step in the coarse grid region of the RRM and that one in the high-resolution domain?

The dynamics use 3 layers of substepping. For the LRM (HRM), the Lagrangian vertical discretization timestep is 15 minutes (2.5 minutes), the horizontal discretization timestep is 5

minutes (75 seconds), and the explicit numerical diffusion timestep is 100 seconds (18.75 seconds). In RRM, the same time steps are used for both the low- and high-resolution domains. The RRM_LR simulation uses the LRM time steps, while other RRM simulations use the HRM steps. We have revised the manuscript to include this dynamic timestep information on page 5.

3. Page 5, line 30 -34 "All free-running simulations are run for a period of 5 years. The first year is considered spin-up, thus we study the results from the last 4 years. The nudging run simulates year 2011, whereas the AMIP results are extracted for year 2011 from a long simulation starting from 1870 (Golaz et al., 2019). Model output is stored as monthly and hourly averages." This is the only part in the manuscript where I can find an information on the time period. From Table 2 it seems that all observations have different time periods. Are the time periods listed there are also the time periods which are compared with the model results?

This is correct. In this study, we mainly focus on the modeled climatologies. The time periods listed in Table 2 are used to calculate the observed climatologies to compare with the model results.

4. Page 13, line 9-11 "... incorrect diurnal cycles. The similarity between RRM and HRM indicates that RRM simulations will be valuable for understanding and addressing this important model bias." and line 28-31 "... the time of peak precipitation is a few hours early, consistent with the experience of other models. More physically based improvements are needed to find a solution to the summertime diurnal cycle issue for precipitation over the CONUS, and the RRM provides an efficient tool for parameterization testing."

As the authors state right this is a well-known problem of coarse grid models. However, they did not cite any papers on possible solutions.

A possible solution for the ECMWF convection scheme is described in BECHTOLD, P., SEMANE, N., LOPEZ, P., CHABOUREAU, J.-P., BELJAARS, A., BORMANN, N., 2014: Representing Equilibrium and Nonequilibrium Convection in Large-Scale Models. *Journal of the Atmospheric Sciences* 71, (Heft 2), S. 734–753.

In general this problem does not appear in convection permitting simulations (< about 2-4 km grid width). A starting point for reading on the effect of convective permitting simulations on the diurnal cycle: PREIN, A. F., LANGHANS, W., FOSSER, G., FERRONE, A., BAN, N., GOERGEN, K., KELLER, M., TOELLE, M., GUTJAHR, O., FESER, F., BRISSON, E., KOLLET, S., SCHMIDLI, J., VAN LIPZIG, N. P. M., LEUNG, R., 2015: A review on regional convection-permitting climate modeling: Demonstrations, prospects, and challenges. *Reviews of Geophysics* 53, (Heft 2), S. 323–361.

In general the authors seem not be very familiar with articles written in Europe.

Thanks for pointing out this important information we missed in our manuscript. At the end of Section 3, we added the following text and references.

Previous studies (e.g., Bechtold et al., 2004; Stratton and Stirling, 2012; Bechtold et al., 2014) provide possible solutions for this issue of simulating the diurnal cycle of convective precipitation over land by modifying convective trigger procedures, entrainment, and convective closures. Our recent study (Xie et al., 2019) shows substantial improvement in the

precipitation diurnal cycle in the LRM by employing a new convective trigger with a dynamic constraint on the convection onset, and with the capability of detecting moist instability above the boundary layer. We will apply the RRM testbed to extend the new convective trigger to the HRM and report the results in a future paper. This bias in the diurnal cycle of convection is significantly improved in convection-permitting (horizontal grid spacing < 2-4 km) simulations (Prein et al., 2015). The E3SM project is making progress in developing its convection-permitting version (E3SMv4), for which the RRM testbed will be heavily relied on.

5. Figures 5-11 Please add to each of the figures an additional one showing the absolute values of the observations. Otherwise it is hard to judge whether biases are large or small.

We added the observation plots as panel (e) on these figures. We also reversed the colormap for the difference plots of precipitation and total precipitable water – blue represents wetter, while brown drier.

6. Figure 10 The authors write in the text (page 10, line 30) "... LRM simulation exhibits statistically significant positive temperature (up to 3 K) biases throughout the area (see Fig. 10a), ..." (meaning biases to ERA-Interim). From the the biases of HRM and RRM are then even larger compared to ERA-Interim (Fig. 10b up to 6 K and the same in Fig. 10c, but for a smaller region). These are quite large biases. Can the authors give any explanation why the temperature bias doubles for the high-resolution model versions?

The warm bias can be roughly attributed to two separate sources: the evaporative fraction (EF) contribution and the radiation contribution which is primarily caused by excessive absorbed solar radiation at the surface. EF is defined as the fraction of the combined latent and sensible heat fluxes that are in latent form. Models with too low EF tend to use the radiative input to heat the surface instead of evaporating water (Ma et al., 2018).

We applied the diagnostic (Equation 1 of Ma et al., 2018) to our model results and found that the larger temperature bias in the high-resolution model versions is because the EF contribution is a few times larger with enhanced resolution, while the radiation contribution remains almost unchanged.

We added the following in this paragraph. "This warm bias can be roughly attributed to two separate sources (Ma et al., 2018): the evaporative fraction (EF) contribution and the radiation contribution which is primarily caused by excessive absorbed solar radiation at the surface. EF is defined as the fraction of the combined latent and sensible heat fluxes that are in latent form. Models with too low EF tend to use the radiative input to heat the surface instead of evaporating water. The larger bias in the HRM is because the EF contribution is a few times larger with enhanced resolution, while the radiation contribution remains almost unchanged."

Technical Corrections

1. Figure 15 Please enlarge the legend circle at the top right and add an additional radius axis with precipitation values.

We revised Figure 15 with the enlarged legend circle. Now the legend text and the radius axis inside the circle are shown clearer.

Anonymous Referee #2

The authors of the reviewed manuscript present a framework for testing physics parametrizations on their scale awareness. They analyse the differences in a globally refined model (RRM) against a global high-resolution model (HRM). The advantage of a refined model lies in the computational cost. The authors state that the RRM model can mimic the outcome of the HRM model and can be used for future developments. Here, a selected area over the United States (CONUS) is used for the model evaluation. The authors compare the model results, both of HRM and RRM against measurements. The focus is set on hydrological values as precipitation. In addition, the authors focus on variables suitable for dynamical characterisation.

The manuscript needs major revisions. First of all, the category of this paper should be revised. As stated on the web page for manuscript types: https://www.geoscientific-model-development.net/about/manuscript_types.html#item2 Development and technical papers should include details about the model improvements in terms of speed or accuracy. Here, some additional benchmarks in terms of computational time are missing. In addition, while reading the manuscript, I got the overall impression, that the authors are focussing more on the used parameterizations, than the code development. This focus has to be shifted, in order to address the demands of this specific manuscript type.

We agree that the manuscript needs to be revised to better fit the “development and technical” category. We made the following major changes:

- Added the model speed and cost information in Table 1 to benchmark the RRM computational performance and highlight its computational efficiency relative to the uniform high-resolution model.
- Revised the title to “Regionally refined testbed in E3SM Atmosphere Model Version 1 (EAMv1) and applications for high-resolution modelling” to emphasize the RRM technical usage as a physics parameterization testbed for high-resolution modelling.
- We included more information about the code development of implementing the RRM.

The overall objective is also a bit vague. Based on the abstract only, I can get three objectives. These are climate applications, usage as a testbed for physics parametrisations and hydrologic research. These are three points only discussed in a shallow way. I suggest to aim for the point of testbed usage. Here, the side by side comparisons shown in the result section would gain weight and the authors could discuss a bit more how to tackle occurring obstacles in the RRM model against HRM.

We tried to state the overall goal of this paper as clearly as possible, but we agree it can be improved. We like the suggestion of aiming for the testbed usage. As mentioned above, the title was changed to explicitly point out RRM as a testbed. We also revised the whole text to focus on the testbed point. For instance, the last sentence of the abstract was revised to "...the RRM is an efficient and effective testbed for HRM development", and the last sentence of the first paragraph of Section 2.1 was changed to "...we focus on the EAMv1 regionally refined testbed capability over the CONUS domain".

The introduction is a bit packed with acronyms. It is a overwhelming while reading the manuscript for the first time. In general, I would recommend a table of acronyms in the end. Plus, it would end in a better readability if less acronyms would be used. The results you show are limited do DJF and JJA. I suggest to provide other seasons as well and at least discuss why you are not using these seasons for more intense studies. The last general point is, that I would wish for a detailed description of the technical implementation of the RRM.

Thanks for the suggestion. We included the acronym table (Table 4) in the revised version as suggested. Regarding the description of the technical implementation of the RRM, we added the following in the second paragraph of Section 2.1, "We created the regionally refined grid with the offline software tool, Spherical Quadrilateral Grid Generator (SQuadGen, <https://github.com/ClimateGlobalChange/squadgen>)." and "We used a new tensor hyperviscosity formulation (Guba et al., 2014) to eliminate numerical noise and oscillations."

Our main purpose here is to document the RRM testbed with "proof-of-concept" examples instead of an intense study. The DJF and JJA are the two extreme seasons, while MAM and SON are more moderate with the results somewhat in between DJF and JJA. Therefore, we chose to only show DJF and JJA. We added this reason at the beginning of the results section (Section 3) as "In this section, we will focus on the results of June-July-August (JJA) and December-January-February (DJF), the two more extreme seasons at the CONUS in a year when some long-standing systematic model errors are present."

After the major revision, the manuscript may be published in GMD.

Specific comments:

1. P1L13 [. . .] process-level representation at finer resolutions is a pressing need in order [. . .]. Could you please add a number here? What means finer? Finer than . . . ?

We added "< 100 km" in the sentence. The specific resolution requirements vary by the extreme events that the policies target. 100 km is a typical resolution used in the current climate simulations and is often too coarse.

2. P1L14 [. . .] regarding extreme events in a changing climate. This is a bit too vague. Why do model simulations in a higher resolution provide more information to policy makers? I would suggest to rewrite the start of the abstract to get a bit more precise.

We revised the sentence to "... in order to provide more detailed actionable information...". Extreme events often occur at high spatial and temporal scales. High-resolution simulations can provide more details about these events than can the low-resolution simulations.

3. P1L22/23 *Differences between the RRM and HRM over the HR region are predominantly small, demonstrating that the RRM reproduces both well- and poorly simulated behaviours of the HRM over the CONUS.*

Again, too vague. In addition, the phrasing is a bit misleading. Roughly speaking, you have the same errors in both models. Please, rephrase.

Thank you, we have adjusted the text to be clearer.

4. P1L25 *influenced by the different parameter choices[. . .]*

This is a statement that is very obvious. I won't mention that in an abstract.

Considering one of the most important applications of RRM as a testbed is to test the model performance with different parameters, we prefer to keep this sentence.

5. P1L31 *[. . .] hydrologic research.*

No given context.

Removed. Thanks.

6. P2L4 *finer in the horizontal*

Finer means xx degrees?

At the end of this paragraph, we mentioned that the E3SM plans to develop global cloud-resolving model with 3 km resolution. Finer means the resolution between 3 km and 25 km.

7. P2L6 *and they must often be done at HR.*

I suggest to remove that part of the sentence.

Deleted.

8. P2L8 *one-year HR (0.25 average)*

Already defined - please erase

We changed to "one-year 0.25° HR". It is worth mentioning the resolution here to avoid confusion.

9. P2L12-15 *The RRM simulation cost is usually dominated by the computational cost of the HR region, and thus the total model cost is roughly proportional to the size of the region with finer resolution, referred to as a "mesh" (typically chosen to be about 10% of the globe, making the cost about 10% of a uniform HRM simulation.*

This is a bit self explanatory. Could you please include more details about the load balancing, computational costs, scaling factors and memory efficiency?

Thank you for the suggestions. We feel that this sentence is probably useful for the audience who are less familiar with the RRM to gain a rough idea about how much RRM can save relative to the uniform high-res model. We prefer to keep it.

We added details about the speed (simulation years per day), node numbers, and the cost (core-hours per year) of all the model settings used in this study in the revised Table 1 to give more information about the technical aspects of the model. It shows that in the simulations analyzed here the RRM cost is 13%-15% of the uniform high-res model, depending on the parameter choices.

10. P2L16 *E3SMv2 science goals*
Please explain.

The manuscript has been revised to include more details: "...E3SMv2 science goal of understanding the relative impacts of global forcing versus regional influences of human activities on flood and drought in North America."

11 P2L20 *with 3 km horizontal grid*
Please be consistent with the units here. You've started with degrees, now switching to km.

Traditionally, degrees are used for coarse resolution global models and km for cloud-resolving models. We switched the units to be consistent with this convention.

12 P3L5 *play in future E3SM scientific and energy applications*
The aspect of energy application just pop up right here. Could you please describe those in more detail?

We changed the sentence to "...in future E3SM scientific applications".

13 P3L12 *when increasing model resolution.*
You mean the horizontal resolution?

We meant both the horizontal and vertical resolutions. Changed to "when increasing model horizontal or vertical resolution."

14 P3L30-32
related to fast physics [. . .] [. . .] to fast physics, such as clouds and precipitation.
Please add a careful definition of fast and slow physics here.

We added the definitions of fast vs. slow physics by revising the text to "...between short (a few days) and long (seasonal to annual) timescale systematic errors in climate models...".

15 P4L15-20 This paragraph is much too long. The phrasing of e.g. “higher” should be more precise, e.g. higher than . . .

We changed the text to read “a higher (~ 0.1 hPa compared to 2 hPa) model top”.

16 P4L26 Here, you name the definition of LRM and HRM again. Just leave that out.

Done. Thanks.

17 P4L29 [. . .] *tested over the Tropical Western Pacific (TWP) and the Eastern North Atlantic (ENA)*
Why is that worth mentioning?

This paper serves as the main documentation of the EAMv1 RRM, so we think it is worth pointing out the available RRM grids over other regions in EAMv1.

18 P5L19 [. . .] *associated with fast atmospheric physical processes.*
As mentioned above, a careful definition of fast and slow physics would be good.

Agreed. We defined the timescales of fast and slow physics as suggested (see above).

19 P5L31 I’m not fully convinced here, that 5 years of simulation is really an appropriate time frame in terms of statistical significance. You also started your manuscript pin pointing to the climate aspect. While doing five years of simulation, the climate aspect is not covered what so ever. If you want to go more in the direction of the climate simulation, there is a need for a better discussion either why five years are really sufficient or perform more simulations. Thinking about ensemble, timeslice or just longer time periods.

The reasons why 5 years simulations are appropriate are because our present study focuses on hydrological variables, for example precipitation, and we mainly use the atmosphere-only simulations with cycling climatologically forcings and emissions.

Previous studies (Xie et al., 2012; Ma et al., 2014) have demonstrated a strong correspondence between short and long timescale systematic errors in climate models for fields related to fast physics, such as precipitation and clouds. We verified this finding with a 20-year LRM simulation and found that the 5-year climatology and 20-year climatology of the variables analyzed here are very similar. Also considering the expensive cost of multi-decadal HRM simulations, we opted to use 5-year simulations for all resolutions.

20 P6L1 No need for the wording “skilful” here.

We want to emphasize the link between better model skills and more realistic simulation. We intend to keep it.

21 P6L18 How did you do this selection? Please describe the criteria you've chosen.

We mainly follow the Program for Climate Model Diagnosis and Intercomparison (PCMDI) Metrics Package (PMP). We added the citation to Gleckler et al. (2016).

22 P6L24 *model results are conservatively interpolated*

What do you mean by conservatively? Please add more details on the interpolation method.

We used the "conserve" method of the Earth System Modeling Framework (ESMF) regridding software. The text was revised to "model results are conservatively interpolated (with the "conserve" method of the Earth System Modeling Framework (ESMF, <https://www.earthsystemcog.org/projects/esmf/>) regridding software) to..."

23 P6L30 This sentence is way too self explanatory.

That is true, but we received feedback from the readers that they somehow thought the goal of our analysis is to show the RRM outperforms the HRM. We, therefore, decided to make it clear.

24 P7L10 Why does the land surface model behave so differently? Please comment on that and add more details to that finding.

This is mainly due to the different surface energy partitioning in the land surface models. The fraction of sensible heat flux is much higher in the HRM than in the LRM. Please see the response to question 6 of the specific comments of reviewer #1 for details.

We changed the sentence to "...along with feedbacks (surface energy partitioning shifting towards more sensible heat flux) from the land surface model."

25 P7L33 Please elaborate on the point of improved physical processes.

Changed to "...improved representation of physical processes by better physical parameterizations."

26 P10L16-21 I do miss numbers in this paragraph. Please provide additional information if you use the phrase too strong or relatively small.

We included the numbers where strong or small are used in this paragraph.

27 P12L13 I'm missing additional information about the interpolation method.

The interpolation method was provided as "...are interpolated with the ESMF conservative regridding method to..."

28 P13L8 Do you have any strategies of tackling that problem, that the model is not able to represent the night time maximum?

A new convective trigger can help reduce this night time precipitation bias. The new trigger uses a dynamic constraint on the convection onset and has the capability of detecting moist instability above the boundary layer. The details about this recent study was reported by Xie et al., (2019).

29 P13L29 other models Any references? What other models do you mean?

We added the references to Dai et al., 1999; Stratton and Stirling, 2012; Bechtold et al., 2014 for the NCAR regional climate model, Met Office Hadley Centre climate model, and the ECMWF model.

30 P13L31 efficient tool for parameterization testing This is an interesting point. I'm strongly encouraging you in working on that aspect a bit more and provide more details.

The RRM is much more efficient than the HRM in terms of its computational cost, throughput, and storage requirements. Our revised Table 1 includes the speed and cost details for RRM and HRM. It clearly shows that the RRM only costs 15% of the HRM with a 15% faster throughput and requires much less (13%) compute nodes.

31 P15L11 Do you really mean many, or just those two?

Deleted "many".

32 P15L25 I disagree that the only conclusion is to develop better scale aware parameterizations. There are also model developments were you end up having e.g. convection permitting simulations.

Revised to "...the need to develop better scale-aware physical parameterizations or convection-permitting simulations in the future."

33 P15L28 I'm a bit confused about the phrase detailed guidance, could you please comment on that?

We included Table 3 with all the parameters for the non-US nudging simulation analyzed in this paper as an example for users who are interested in running EAMv1 RRM with nudging.

Technical comments

P1L12 Climate simulation => Plural please

Corrected. Thanks.

P3L2 all => All Make it two sentences

Done.

P5L7 analysed vs. analyzed

GMD requires the British spelling “analysed”.

P5L26 nudging => nudged

Done.

P5L31 considered as spin-up

Thank you. Done.

P11L32 overwhelming is not a proper term here.

Revised to “dominant”.

P14L32 analysed vs. analyzed

See above.

P20L18 Please check you bibliography => N/A N/A

The page information was corrected.

P22L14 Please add a date of last access.

Done

Figure 1, 12 and 13 should be enlarged.

We changed Figure 1. We will enlarge Figures 12 and 13 during the typesetting process.

Reference:

Bechtold, P., Chaboureaud, J.-P., Beljaars, A., Betts, A. K., Köhler, M., Miller, M. and Redelsperger, J.-L.: The simulation of the diurnal cycle of convective precipitation over land in a global model, Q. J. R. Meteorol. Soc., 130(604), 3119–3137, doi:10.1256/qj.03.103, 2004.

Bechtold, P., Semane, N., Lopez, P., Chaboureaud, J.-P., Beljaars, A. and Bormann, N.: Representing Equilibrium and Nonequilibrium Convection in Large-Scale Models, *J. Atmospheric Sci.*, 71(2), 734–753, doi:10.1175/JAS-D-13-0163.1, 2014.

Ma, H. -Y., Klein, S. A., Xie, S., Zhang, C., Tang, S., Tang, Q., et al. (2018). CAUSES: On the Role of Surface Energy Budget Errors to the Warm Surface Air Temperature Error Over the Central United States. *Journal of Geophysical Research: Atmospheres*, 123(5), 2888–2909. <https://doi.org/10.1002/2017JD027194>

Ma, H.-Y., Xie, S., Klein, S. A., Williams, K. D., Boyle, J. S., Bony, S., Douville, H., Fermepin, S., Medeiros, B., Tyteca, S., Watanabe, M. and Williamson, D.: On the Correspondence between Mean Forecast Errors and Climate Errors in CMIP5 Models, *J. Clim.*, 27(4), 1781–1798, doi:10.1175/JCLI-D-13-00474.1, 2014.

Gleckler, P., Doutriaux, C., Durack, P., Taylor, K. E., Zhang, Y., Williams, D., Mason, E. and Servonnat, J.: A more powerful reality test for climate models, *Eos Trans. Am. Geophys. Union*, 97, doi:10.1029/2016EO051663, 2016.

Guba, O., Taylor, M. A., Ullrich, P. A., Overfelt, J. R. and Levy, M. N.: The spectral element method (SEM) on variable-resolution grids: evaluating grid sensitivity and resolution-aware numerical viscosity, *Geosci. Model Dev.*, 7(6), 2803–2816, doi:<https://doi.org/10.5194/gmd-7-2803-2014>, 2014.

Prein, A. F., Langhans, W., Fosser, G., Ferrone, A., Ban, N., Goergen, K., Keller, M., Tölle, M., Gutjahr, O., Feser, F., Brisson, E., Kollet, S., Schmidli, J., Lipzig, N. P. M. van and Leung, R.: A review on regional convection-permitting climate modeling: Demonstrations, prospects, and challenges, *Rev. Geophys.*, 53(2), 323–361, doi:10.1002/2014RG000475, 2015.

Stratton, R. A. and Stirling, A. J.: Improving the diurnal cycle of convection in GCMs, *Q. J. R. Meteorol. Soc.*, 138(666), 1121–1134, doi:10.1002/qj.991, 2012.

Xie, S., Ma, H.-Y., Boyle, J. S., Klein, S. A. and Zhang, Y.: On the Correspondence between Short- and Long-Time-Scale Systematic Errors in CAM4/CAM5 for the Year of Tropical Convection, *J. Clim.*, 25(22), 7937–7955, doi:10.1175/JCLI-D-12-00134.1, 2012.

Xie, S., Wang, Y.-C., Lin, W., Ma, H.-Y., Tang, Q., Tang, S., Zheng, X., Golaz, J.-C., Zhang, G. and Zhang, M.: Diurnal Cycle of Precipitation Simulated by E3SM with a Revised Convective Trigger, *J. Adv. Model. Earth Syst.*, submitted, 2019.

Regionally refined testbed in E3SM Atmosphere Model Version 1 (EAMv1) and applications for high-resolution modelling

Deleted: capability

Qi Tang¹, Stephen A. Klein¹, Shaocheng Xie¹, Wuyin Lin², Jean-Christophe Golaz¹, Erika L. Roesler³, Mark A. Taylor³, Philip J. Rasch⁴, David C. Bader¹, Larry K. Berg⁴, Peter Caldwell¹, Scott Giangrande², Richard Neale⁵, Yun Qian⁴, Laura D. Riihimaki⁴, Charles S. Zender⁶, Yuying Zhang¹, and Xue Zheng¹

¹Lawrence Livermore National Laboratory, Livermore, CA 94550, USA

²Brookhaven National Laboratory, Upton, NY 11973, USA

³Sandia National Laboratory, Albuquerque, NM 87185, USA

⁴Pacific Northwest National Laboratory, Richland, WA 99352, USA

⁵National Center for Atmospheric Research, Boulder, CO 80305, USA.

⁶Departments of Earth System Science and Computer Science, University of California, Irvine, Irvine, CA 92697, USA

Correspondence to: Qi Tang (tang30@llnl.gov)

Abstract. Climate simulations with more accurate process-level representation at finer resolutions (< 100 km) is a pressing need in order to provide more detailed actionable information to policy-makers regarding extreme events in a changing climate. Computational limitation is a major obstacle for building, and running high-resolution (HR, here 0.25° average grid spacing at the equator) models (HRM). A more affordable path to HRM is to use a global regionally refined model (RRM), which only simulates a portion of the globe at HR while the remaining is at low-resolution (LR, 1°). In this study, we compare the Energy Exascale Earth System Model (E3SM) atmosphere model version 1 (EAMv1) RRM with the HR mesh over the contiguous United States (CONUS) to its corresponding globally uniform LR and HR configurations, as well as to observations and reanalysis data. The RRM has a significantly reduced computational cost (roughly proportional to the HR mesh size) relative to the globally uniform HRM. Over the CONUS, we evaluate the simulation of important dynamical and physical quantities as well as various precipitation measures. Differences between the RRM and HRM over the HR region are predominantly small, demonstrating that the RRM reproduces the precipitation metrics of the HRM over the CONUS. Further analysis based on RRM simulations with the LR vs. HR model parameters reveals that RRM performance is greatly influenced by the different parameter choices used in the LR and HR EAMv1. This is a result of the poor scale-aware behaviour of physical parameterizations, especially for variables influencing sub-grid scale physical processes. RRM can serve as a useful framework to test physics schemes across a range of scales, leading to improved consistency in future E3SM versions. Applying nudging-to-observations techniques within the RRM framework also demonstrates significant advantages over a free-running configuration for use as a testbed, and as such represents an efficient and more robust physics testbed capability. Our results provide additional confirmatory evidence that the RRM is an efficient and effective testbed for HRM development.

Deleted: both well- and poorly simulated behaviours

Deleted: approach

Deleted: and hydrologic research

1 Introduction

A key goal of the United States (US) Department of Energy (DOE) Energy Exascale Earth System Model (E3SM) project (formally known as the Accelerated Climate Modeling for Energy (ACME)) is to develop a high-resolution (HR, 0.25° or finer in the horizontal) fully-coupled Earth system model for climate simulation and prediction (Bader et al., 2014). Testing new physical parameterizations and tuning loosely constrained parameters within existing parameterizations are important steps of model development. However, the computational cost of running a globally uniform HR model (HRM) is high. For example, a one-year 0.25° HR E3SM Atmosphere Model Version 1 (EAMv1) simulation requires 0.6 million core-hours on 675 "Knights Landing" (KNL, Intel Xeon Phi Processor 7250) nodes of the Cori supercomputer at the National Energy Research Scientific Computing Center (NERSC). A regionally refined model (RRM) capability (Ringler et al., 2008; Zarzycki and Jablonowski, 2014; Roesler et al., 2018), which only simulates a fraction of the globe at HR, is adopted by EAMv1 to reduce the computational cost of HR simulations and to examine the parameterization sensitivity to HR scales. The RRM simulation cost is usually dominated by the computational cost of the HR region, and thus the total model cost is roughly proportional to the size of the region with finer resolution, referred to as a "mesh" (typically chosen to be about 10% of the globe, making the cost about 10% of a uniform HRM simulation). In the ongoing E3SM phase II project, the RRM configuration is planned as a central tool to achieve the E3SMv2 science goal of understanding the relative impacts of global forcing versus regional influences of human activities on flood and drought in North America. RRM will be routinely used over North America to address DOE's goal to understand the Earth system changes affecting US energy-sector decisions. It will be also applied as a physics testbed to improve the scale-awareness of parameterizations in upcoming versions of E3SMv2 and v3 as well as an important strategy to perform larger ensemble of HR simulations. RRM is also a vital capability for progress towards an eventual global cloud-resolving model with 3 km horizontal grid spacing targeting E3SMv4 and beyond.

The RRM approach has been established and validated with other models over many regions of interest. For instance, Zarzycki et al. (2014) showed the effectiveness of an RRM with aquaplanet experiments using the Community Atmosphere Model (CAM). Zarzycki and Jablonowski (2014, 2015) demonstrated improved skill in simulating tropical cyclones in CAM with a refined mesh over the North Atlantic. Rhoades et al. (2016) and Wu et al. (2017) depicted that the variable-resolution (VR) Community Earth System Model (CESM) was able to accurately capture the climatology and seasonality of important variables over mountain regions. Huang and Ullrich (2017) reproduced the geographic patterns of historical precipitation climatology over the western US with the VR-CESM. Gettelman et al. (2018) performed comprehensive tests of a VR dynamical core in CESM2 and showed that VR grids were feasible alternative to conventional nesting for regional climate research. Roesler et al. (2018) found that refining the grid over the contiguous United States (CONUS) did not exert a noticeable influence on the global circulation in the EAM version 0 (EAMv0, which is almost identical to CAM5.3 except

Field Code Changed

Deleted: , and they must often be done at HR

Deleted: HR (

Deleted: average grid spacing at the equator)

Deleted: 9

Deleted: 512

Deleted: s

Field Code Changed

for some minor tunings and bug fixes). These earlier studies have demonstrated that RRM can be used as an effective tool to study important climate features over regions of interest with high resolution.

Compared to EAMv0, EAMv1 (Rasch et al., 2019) includes significant changes to its physics, substantially increased vertical resolution, retuning, and bug fixes (Zhang et al., 2018). All these changes cause the model to behave very differently from EAMv0, especially in terms of regional clouds and precipitation characteristics (Xie et al., 2018). Given these substantial model changes and the critical role that RRM will play in future E3SM scientific applications, this paper documents further scientific analysis of RRM behaviour with EAMv1. We contrast simulations between the RRM and the globally uniform HR EAMv1 over the RRM region, with the goal to provide more insights into the EAMv1 RRM capability to the user community. This study emphasizes hydrology-related simulation skill over North America: a key element of the E3SM Water Cycle science driver. We investigate whether RRM reproduces the same performance as HRM of these fields enabling it to be used as an effective physics testbed for understanding physical processes and improving their representations in EAMv1 and in future versions. In addition, EAMv1 physical parameterizations (and in particular the cloud parameterizations) are not inherently scale-aware and hence require retuning when increasing model horizontal or vertical resolution. Unfortunately, this leads to two different parameter settings for EAMv1 high- and low-resolution models. It is key to determine how the two different parameter settings influence RRM performance, since most earlier studies just used the established low-resolution model parameters over the RRM domain, which may not yield optimal RRM results due to scale-aware shortcomings of the existing physical schemes.

This study centres mainly on “proof-of-concept” examples. More in-depth analysis of RRM behaviour will be reported in separate studies when RRM is more routinely used in E3SM phase II and by general users. In many EAMv1 application scenarios, it is expected that the RRM will be more feasible and practical than the HRM. This could include evaluation against regional measurements, uncertainty quantification studies that typically demand a large ensemble size (Qian et al., 2016, 2018), and users with limited computational resource. Findings from this study regarding the strengths and weaknesses of the EAMv1 RRM configuration should provide valuable guidance for future RRM applications in the HR E3SM development and broad community use of the E3SM RRM.

Additionally, we provide detailed information on how to utilize the RRM capability with nudging for process-level understanding of model deficiencies. Similar to the hindcast approach (Phillips et al., 2004; Ma et al., 2015) used in climate model evaluation, the nudging approach is able to maintain the large-scale dynamical state close to an observed state, and hence provides a better assessment of atmospheric physics performance. This nudged approach is particularly useful for those processes that are related to fast physics. Xie et al. (2012) and Ma et al. (2014) demonstrated a strong correspondence between short (a few days) and long (seasonal to annual) timescale systematic errors in climate models for fields related to fast physics, such as clouds and precipitation.

Deleted: (Zhang et al., 2018c),

Deleted: all

Deleted: of which

Deleted: and energy

This paper is organized as follows. Section 2 provides an overview of the RRM EAMv1 and summarizes the setup of simulations and the observational datasets used for model evaluation. Results are shown in Section 3, including model climatologies over the CONUS domain where our RRM has its fine-resolution mesh, the analysis of quantities related to hydrological cycle, and an in-depth analysis of precipitation characteristics – the large-scale/convective partitioning, the intensity distribution, and the summertime diurnal cycle. Section 4 describes an example of running the nudged RRM. Section 5 provides a summary of this work and prospects for future studies.

2 Methodology

2.1 Model overview and experiment design

The E3SM project aims to build a global HR fully-coupled Earth system model for climate simulation and prediction on current and next-generation supercomputing facilities (Bader et al., 2014). Since all the simulations analysed here are atmosphere-only ones, we only provide information about the atmosphere model. Details about the coupled E3SM model can be found in (Golaz et al., 2019). EAMv1 originated from CAM5.3 (Neale et al., 2012), but has undergone substantial development. An overview of EAMv1 is given by Rasch et al. (2019). More details on the simulated cloud and precipitation characteristics and overview of the low- and high-resolution model tunings are provided in Xie et al. (2018). EAMv1 uses the spectral element dynamical core (Taylor and Fournier, 2010; Dennis et al., 2012) on a cubed-sphere computation grid with an explicit Runge-Kutta time integration scheme. This dynamical core has sustained scalability with increasing number of elements and processors (Fournier et al., 2004). Major changes in EAMv1 compared to its earlier version include substantially increased vertical resolution (72 vs. 30 vertical layers), a higher (~0.1 hPa compared to 2 hPa) model top, and improved physical parameterizations including the Cloud Layers Unified By Binormals (CLUBB) scheme (Golaz et al., 2002; Bogenschutz et al., 2013), updated cloud microphysics (MG2) (Gettelman and Morrison, 2015), predicted aerosols (the Modal Aerosol Module (MAM4)) (Liu et al., 2016), and a linearized ozone chemistry (Linoz2) (Hsu and Prather, 2009). Impacts of the new cloud physics and the increase in vertical resolution on EAMv1 simulated climate are documented in Xie et al. (2018) and Qian et al. (2018). In the present paper, we focus on the EAMv1 regionally refined testbed capability over the CONUS domain.

The CONUS regionally refined grids consist of LR and HR regions and a transition area between them (see Fig. 1a). The HR grid is located in the CONUS area. We created the regionally refined grid with the offline software tool, Spherical Quadrilateral Grid Generator (SQuadGen, <https://github.com/ClimateGlobalChange/squadgen>). The effective resolutions for the LR and HR regions are 1° and 0.25°, respectively. Because of the horizontal resolution differences in the LRM, the HRM, and the RRM, the topography is represented differently in these configurations. We used a new tensor hyperviscosity formulation (Guba et al., 2014) to eliminate numerical noise and oscillations. Additional details about the CONUS RRM as

Field Code Changed

Field Code Changed

Field Code Changed

Field Code Changed

Field Code Changed

Field Code Changed

Field Code Changed

Field Code Changed

Deleted: (~1° horizontal grid spacing)

Deleted: (~0.25° grid spacing)

well as the topography data are reported in Roesler et al. (2018). It is worth mentioning that the RRM grids have also being generated and tested over the Tropical Western Pacific (TWP) and the Eastern North Atlantic (ENA).

In the present study, we mainly analyse the atmosphere-only simulations (see Table 1 and A1) forced by observed present-day climatologies of aerosol emissions, greenhouse gases, sea surface temperatures (SSTs) and sea ice concentrations. The simulations use an interactive E3SM land model on the same grids as the atmosphere. We run the EAMv1 with globally-uniform LR and HR grids as well as the CONUS RRM grid. All simulations are performed with the 72 vertical layers. Since the EAMv1 parameterizations are not scale-aware, both dynamical and physical parameters are adjusted to optimize the model performance at different resolutions (Xie et al., 2018). This leads to different parameter settings for the EAMv1 LRM and HRM. As shown in Table A1 of Xie et al. (2018), the differences are mainly in parameters that control convection and cloud microphysics. Thus, differences between LRM and HRM analysed in the following sections arise from different horizontal resolutions and parameter settings, as well as the different physics time steps. The LRM and HRM physics time steps are 30 minutes and 15 minutes, respectively. The dynamics use 3 layers of substepping. For the LRM (HRM), the Lagrangian vertical discretization timestep is 15 minutes (2.5 minutes), the horizontal discretization timestep is 5 minutes (75 seconds), and the explicit numerical diffusion timestep is 100 seconds (18.75 seconds). The RRM uses the same dynamics time steps over the LR and HR domains. For the purpose of mimicking the HRM behaviours, we opt to use the same dynamical and physical parameters and time step for the RRM control simulation as in the HRM. Besides the RRM control case, we also perform an RRM test (RRM_LR) with the LRM dynamical and physical parameters. Comparing these two RRM results, we are able to explore the impact of different parameter settings on the RRM performance, which is not possible for conventional RRM studies with only the LR parameters.

Current climate models commonly suffer from systematic biases in simulating climate mean states of clouds and precipitation associated with flaws in physical parameterizations (e.g., Klein et al., 2013; Ma et al., 2014). However, compensating errors from nonlinear feedback mechanisms also contribute to climate mean biases, making it a challenge to pin the errors to specific parameterizations. The numerical weather prediction technique (Phillips et al., 2004), also known as the transpose-AMIP (Williamson, 2013) or hindcast (Ma et al., 2015) approach, has been increasingly used in climate models, including EAMv1, to understand and reduce model errors associated with fast atmospheric physical processes. Similar to the hindcast method, the EAMv1 RRM can be run in a nudging configuration to diagnose parameterization-related errors and helping to guide development in HR E3SM. More guidance on using the nudged RRM approach will be discussed in Section 4.

To demonstrate the nudging capability, we perform an RRM simulation nudged to the European Centre for Medium-range Weather Forecasting Interim (ERA-Interim) analysis fields of horizontal velocities (U and V) (Dee et al., 2011) with a 6-hour relaxation time scale. The nudged simulation uses the prescribed weekly, 1° spatial resolution SSTs and sea ice from the

Field Code Changed

Deleted: nudging

results, and blue dots RRM results with the HRM parameters. The model results are illustrated relative to the verification data (marked by the reference point (1, 0)) described in Section 2.2. To make consistent comparisons between different model resolutions, model results are conservatively interpolated (with the “conserve” method of the Earth System Modeling Framework (ESMF, <https://www.earthsystemcog.org/projects/esmf/>) regridding software) to the coarser verification data grids before calculating the Taylor statistics. The radial axis shows the geographic variability (i.e., standard deviation (STD)) in the model climatology normalized by that in the observations. The angular axis indicates the spatial correlation (i.e., Pearson correlation coefficient (r)) between the simulations and the observations. By design, the distance to the reference point (1, 0) represents the centred root-mean-square (RMS) difference between the simulated and observed patterns normalized by the STD of the observations. The closer distance to the (1, 0) point, the better the model performance. We should note that the primary purpose of our analysis is to show how well the RRM, as an analogue to the HRM, reproduces the HRM results. The observations and the LRM results provide quantitative references to examine the RRM-HRM similarity and also identify poorly simulated behaviours as targets of HRM development.

Relative to the evaluation datasets (Fig. 2ab), the thermodynamic variables are generally well-simulated by EAMv1 with all three model configurations. All correlation coefficients are greater than 0.85 (mostly > 0.95). Normalized STDs lie close to the 1.0 dashed curve, especially in JJA. The model generally represents these large-scale circulation related quantities better with finer resolution settings, as the red dots (HRM) are usually closer to the (1, 0) point (representing evaluation data) than the corresponding green dots (LRM). Nevertheless, there are a few exceptions, for example, 2-meter air temperature (T_{2m} or TREFHT) in JJA (see Fig. 2a), which is likely associated with cloud and thus surface radiation changes (Van Weverberg et al., 2018), along with feedbacks (surface energy partitioning shifting towards more sensible heat flux) from the land surface model.

More importantly, when using the HRM as the reference point (Fig. 2cd), blue dots (RRM) are located closer to (1, 0) than the green dots (LRM), indicating that the RRM mimics the HRM behaviours quite well. Additionally, we plot the RRM_LR results (purple dots) on Fig. 2cd to illustrate the potential impact of poor scale awareness, which is a common problem for current climate models, on conventional RRM applications. Lacking the tuned HRM parameters, previous RRM studies often heavily rely on LRM parameters and cannot quantify the likely performance deterioration due to the parameter-resolution mismatch. Here we take advantage of having both LR and HR tuned parameters to show the parameter influence on RRM performance. As expected, RRM_LR is generally less-satisfactory than RRM in matching the HRM behaviours (Fig. 2cd), but the extent varies for different quantities. For instance, the 200-hPa zonal wind (U200) is relatively insensitive to parameter changes in RRM configurations in both seasons. These results reflect the large-scale nature of upper troposphere wind fields. In contrast to U200, RRM total precipitable water (TMQ) shows greater sensitivity to parameter settings, since it is more closely related to sub-grid scale physical processes. These results suggest that RRM generally does well in representing large-scale thermo-dynamical behaviours of HRM, but some quantities are sensitive to the choice of

Field Code Changed

Deleted: (Van Weverberg et al., 2018; Zhang et al., 2018a)

LRM or HRM parameter settings. A re-tuning may be needed for the refined region to optimize performance when model physical parameterizations are scale-sensitive. Specifically, for EAMv1, using the HRM parameter setting is recommended when one utilizes the RRM capability.

5 Compared to thermodynamics variables in Fig. 2, the cloud and precipitation variables in Fig. 3 are more sensitive to sub-grid scale parameterizations (e.g., convection, cloud microphysics, and radiation). Similar to Bacmeister et al. (2014), the variables in Fig. 3 are more poorly simulated than those in Fig. 2 in all configurations: they have weaker (0.5-0.9) correlation coefficients, and are further from the (1, 0) point in both seasons (Fig. 3ab). These results are consistent with the idea that improving the simulation of these variables requires both better resolved large-scale circulations and improved
10 representation of physical processes [by better physical parameterizations](#). Figure 3cd demonstrates this idea quantitatively: the LRM-HRM differences become smaller for all variables after refining the CONUS grids (green to purple); the differences are further reduced by changing the parameters to match the HRM values (purple to blue). Nevertheless, our findings are similar: when increasing the resolution, model performance is generally better in DJF (Fig. 3b) and remains the same or slightly degraded in JJA (Fig. 3a); the RRM results follow those of the HRM closer than do the LRM in both
15 seasons (Fig. 3cd). In addition, all variables except total precipitation (PRECT) are more sensitive to the resolution change in winter than in summer (greater LRM-HRM separation in Fig. 3b than in Fig. 3a). For example, the variance of 500-hPa vertical velocity (OMEGA500) is almost independent of resolution in summer but about 50% larger in the HRM configuration than in the LRM in winter, suggesting stronger wintertime circulation and finer scale of resolved dynamics with the HRM configuration.

20 These overall Taylor statistics indicate that the RRM simulation with the HR parameters captures the HRM climatological statistics reasonably well, which provides the basis for potential applications of the RRM to effectively test physical parameterizations and simulate regional climate at high resolutions. In the following sections, we will further evaluate the similarity between the RRM and the HR EAMv1 simulations. We will examine some variables that are closely related to the
25 atmospheric hydrologic cycle with a primary focus on detailed aspects of precipitation, which remains a significant challenge in current climate models and is a major focus application for E3SM.

3.2 Regional geographic patterns

In this section we study whether RRM can reproduce the regional geographic patterns of hydrologic variables simulated by HRM.

3.2.1 Precipitation

Figure 4 shows the geographic pattern of mean total (large-scale + convective) precipitation differences between LRM and GPCP1DD observations, and the differences among model configurations over the CONUS domain in JJA. The differences

Field Code Changed

between the LRM and evaluation data (i.e., panel a) are computed on the evaluation data grid, while those between models (i.e., panels b-d) are computed on the HRM grid. Dotted regions mark where the differences are statistically significant at a 95% confidence level with the two-tailed Student's t-test assuming that each year is an independent sample. EAMv1 global precipitation results are described by Xie et al. (2018). Compared to GPCP1DD observations, the LRM mostly overestimates (up to 3 mm/day) western US precipitation, and underestimates (up to 4 mm/day) eastern and central US precipitation (Fig. 4a). As implied by the similar correlation coefficients of precipitation in Fig. 3a, the mean precipitation pattern exhibits rather uniform spatial changes (especially over land) among different model configurations (Fig. 4b-d). Over land, the HRM and RRM typically produce less precipitation than the LRM (partially due to the model tuning (not shown)) and the HRM rains the least. Differences between the RRM and the HRM are largely insignificant. In regions that pass the significance test, the differences are also relatively small, for instance, < 1 mm/day in the southern central US, and < 2 mm/day in the eastern US.

Figure 5 shows the differences in precipitation climatology patterns for DJF. An obvious change from the JJA results in Fig. 4 is the topographic signatures in differences between HRM and LRM (Fig. 5b), and RRM and LRM (Fig. 5c) over mountain regions in the western US, which are associated with better resolved topography in the RRM and HRM simulations. In addition, the signs of model differences (Fig. 5b-d) are less uniform in DJF than in JJA. Nevertheless, mean precipitation differences between the RRM and the HRM are also small (within ± 2 mm/day), and not statistically significant over most grid cells. Overall, the RRM and HRM EAMv1 produce very similar mean precipitation geographic patterns in both seasons.

Following the COSP evaluation method described by Zhang et al. (2019), cloud fields (not shown here) from the LRM, HRM, and RRM are compared with the observations from ISCCP, MODIS, and CALIPSO. In JJA, all model configurations generally underestimate total cloud amount relative to CALIPSO observations over the CONUS. High thick (optical depth > 9.4) clouds lessen with enhanced horizontal resolution over the western central US, matching the precipitation change pattern over the same region in Fig. 4a. Low clouds along the western coast over the ocean increase noticeably in the RRM and HRM compared to the LRM. In DJF, greater reduction of cloud amount occurs at all levels at the western central US than in JJA with increased resolution. In both seasons, similar to precipitation, the RRM-HRM cloud differences are generally smaller than those for HRM-LRM.

3.2.2 Precipitable water

Figures 6 and 7 show the seasonal mean total precipitable water (TMQ) in JJA and DJF compared with the ERAI reanalysis data. The LRM underestimates the JJA TMQ over most places (see Fig. 6a) except the northwest US, and smaller areas of the eastern US and Mexico, where we observe significantly overestimated precipitation in Fig. 4a. As suggested by the improvement of precipitation with increasing resolution in Fig. 2, the LRM underestimation is generally improved in the

Field Code Changed

Deleted: Zhang et al. (2018b)

HRM (Fig. 6b) and the RRM (Fig. 6c). The mean RRM-HRM differences (Fig. 6d) are mostly positive ($< 4 \text{ kg/m}^2$). This is due to reduction in precipitation in RRM than in HRM outside of CONUS, where the RRM resolution is coarser than that of the HRM.

- 5 In DJF, the LRM TMQ (Fig. 7a) resembles the patterns (overestimation over the western US and underestimation over the eastern US) of precipitation (Fig. 5a) against evaluation data. Such similarity implies that the precipitation biases in winter are directly related to flaws in precipitable water. The RRM and the HRM differ less (mostly statistically insignificant, see Fig. 7d) than their differences with the LRM (Fig. 7bc).

3.2.3 Low-level circulation

- 10 The low-level jet (LLJ) over the Great Plains of the US exerts significant impact on precipitation primarily in summer (Higgins et al., 1997; Pu and Dickinson, 2014). It is responsible for transporting about one-third of the moisture from the Gulf of Mexico to the central US (Helfand and Schubert, 1995). Based on reanalysis data, Higgins et al. (1997) reported connections between the Great Plains LLJ events and regional precipitation anomalies in summer, such as greater precipitation over the north central US and Great Plains and declined precipitation along the Gulf coast and east coast. Here,
15 we examine the 850-hPa horizontal wind speed (Figs. 8 and 9, the difference vectors are shown by colours (magnitudes) and magenta streamlines (directions)) as an example of the low-level circulation.

In summer, the LRM simulates stronger wind than the ERAI reanalysis over a large portion of CONUS, but weaker southerly LLJ at the central US (see Fig. 8a), which contributes to the low precipitation bias in the Great Plains and along the Gulf coast in Fig. 4a. Enhancing resolution significantly strengthens the LLJ (Fig. 8bc), consistent with results presented by

- 20 Berg et al. (2015) for reanalyses with a range of resolutions, and reduces the differences compared to the ERAI reanalysis, since simulations at finer horizontal resolution can resolve the LLJ-related temperature and pressure gradients better than ones at coarser resolution. Contrarily, the overestimation of zonal wind strength over the northeastern US becomes slightly worse with finer resolution. The RRM-HRM (Fig. 8d) difference (mostly within $\pm 0.8 \text{ m/s}$) is generally smaller than that in
25 other panels, especially for the LLJ region over the south-central US.

In winter, we find **about twice** greater wind differences than in summer (note the different colour scales in Figs. 8 and 9). However, the main features remain unchanged, for instance, the LRM also simulates too strong (**mostly $> 1.0 \text{ m/s}$**) zonal winds (Fig. 9a), and the RRM-HRM difference is relatively small (**within $\pm 2.0 \text{ m/s}$**) and mostly insignificant (Fig. 9d). These
30 results suggest that the RRM mimics the low-level circulation of the HRM, including the summertime LLJ. Together with the precipitable water results in the previous section, they imply similar water vapor transport patterns in the RRM and HRM. Therefore, the RRM is a useful tool to study the HR water transport over CONUS.

Field Code Changed

Field Code Changed

Field Code Changed

Field Code Changed

3.2.4 Surface air temperature

Warm and dry model biases over the summertime central US have been studied for more than a decade (Klein et al., 2006), and are still deficient in the current generation of regional and global climate models (Cheruy et al., 2014; Mueller and Seneviratne, 2014; Lin et al., 2017; Ma et al., 2018; Morcrette et al., 2018). Land (soil moisture)-atmosphere coupling plays a key role in causing warm and dry biases (Mo and Juang, 2003; Klein et al., 2006; Lin et al., 2017; Ma et al., 2018; Van Weverberg et al., 2018), and the related precipitation biases.

Figure 10 shows the mean JJA patterns of differences in T_{2m} between the LRM and ERAI data and between three EAMv1 model pairs over CONUS. Over the central US, the LRM simulation exhibits statistically significant positive temperature (up to 3 K) biases throughout the area (see Fig. 10a), corresponding to precipitation low bias (Fig. 4a) in this region. As implied from the Taylor diagram (Fig. 2), performance degrades further (by up to about 4 K) with enhanced resolution. This warm bias can be roughly attributed to two separate sources (Ma et al., 2018): the evaporative fraction (EF) contribution and the radiation contribution which is primarily caused by excessive absorbed solar radiation at the surface. EF is defined as the fraction of the combined latent and sensible heat fluxes that are in latent form. Models with too low EF tend to use the radiative input to heat the surface instead of evaporating water. The larger bias in the HRM is because the EF contribution is a few times larger with enhanced resolution, while the radiation contribution remains almost unchanged. The noisy and large differences in Fig. 10bc over western and central mountain regions are likely associated with topographic differences at different resolutions. Figure 10d shows that the RRM-HRM differences are small (< 2 K) and statistically not significant, but robustly positive over the west coast and negative elsewhere.

Figure 11 shows the T_{2m} results in DJF. The LRM (Fig. 11a) still suffers from warm bias over the central US, but it is less severe and much less widespread than in JJA. Over almost the entire eastern US, the LRM underestimates (by up to 4 K) T_{2m} . The HRM (Fig. 11b) and RRM (Fig. 11c) simulations appear better than the LRM over the Great Plains, the north central US, and the southeastern US. The RRM-HRM differences in Fig. 11d are again the smallest among all panels and statistically insignificant except for the southwestern US.

So far, we have demonstrated that the RRM capability reproduces the characteristics of hydrologic fields simulated in HRM. This proves that the RRM is a reliable ~~testbed~~ which can be used to effectively study and understand these model biases. Next, we will present further analysis on precipitation with RRM and compare it with HRM. Note that the hydrological cycle is a major focus of E3SM of which precipitation is the most important atmospheric variable.

Field Code Changed

Field Code Changed

Deleted: tool

3.3 Precipitation characteristics

3.3.1 Partitioning between large-scale vs. convective precipitation

Precipitation in climate models (e.g., EAMv1) consists of large-scale and convective components. Large-scale precipitation results from condensation due to resolved processes at the model grid resolution and is simulated by the microphysics scheme, while the convective precipitation results from unresolved sub-grid scale processes that are approximated by the deep convection parameterization. Poor partitioning between these two components manifests as errors in the vertical structure of latent heating which corrupts the dynamical response of the environment to convection. Accurately capturing the partitioning is challenging for climate models, which often overestimate the convective component (Lin et al., 2013; Yang et al., 2013). Thus, the partitioning between the large-scale and convective precipitation is an important evaluation metric for climate models. Although they can be clearly defined in the model, the two precipitation components are difficult to separate observationally in a manner comparable to the model. Thus, we only plot the model results for the ratio.

Figures 12 and 13 display the mean ratio of large-scale to total precipitation from EAMv1 models in JJA and DJF, respectively. As expected, convection is a more important source of precipitation in summer and at lower latitudes. The ratio of the large-scale precipitation increases with resolution in Figs. 12 and 13 because more precipitation can be resolved with finer resolution grids and thus classified as large-scale precipitation. Similar convective precipitation changes with resolution are reported by Bacmeister et al. (2014) for CAM4 and CAM5. Consequently, compared to the LRM, large-scale precipitation in the HRM and RRM is more prevalent (especially in the north) during the summer months (see Fig. 12bc) and is even more ~~dominant~~ during the winter months (see Fig. 13bc). In both seasons, the RRM matches the HRM overall distributions of the precipitation partitioning including some regional details, for example, the contour lines along the Sierra Nevada mountains in California in DJF.

3.3.2 Precipitation intensity distribution

Besides the mean precipitation pattern and partitioning between its large-scale and convective components, it is crucial to accurately represent the precipitation intensity distribution in a changing climate, because evidence suggests that extreme events, such as severe storms and flooding, will intensify due to the direct impact of global warming on precipitation (Trenberth, 2011; Seeley and Roms, 2014; Walsh et al., 2014). Like many other global climate models (e.g., Dai, 2006; Stephens et al., 2010; Pendergrass and Hartmann, 2014), Terai et al. (2017) showed that EAMv0 suffers from deficiencies in precipitation intensity over the globe, overestimating the frequency of light to moderate rain compared to the GPCP1DD data.

Figure 14 shows EAMv1 vs. GPCP1DD intensity functions over CONUS in JJA and DJF. Before aggregating the distribution, modelled precipitation rates are interpolated with the ESMF conservative regridding method to the same 1° x 1°

Field Code Changed

Deleted: overwhelming

Deleted: (Trenberth, 2011; Seeley and Roms, 2014; Walsh et al., 2014)

Field Code Changed

Field Code Changed

Field Code Changed

grids as GPCP1DD data. All datasets are averaged over daily intervals. The frequency is then counted in log-bins of precipitation rates on each grid. In this way, the frequency functions from datasets at different spatial and temporal resolutions become comparable. It is evident in Fig. 14 that EAMv1 still simulates excessive light precipitation (< 10 mm/day) with all three configurations in both JJA and DJF. As implied by the mean behaviours in Figs. 12 and 13, convective precipitation accounts for a larger fraction of the total in JJA than in DJF across the whole spectrum (not shown in Fig. 14). Total precipitation from the RRM (blue dots) is closer to the HRM (red dots) than to the LRM (green dots) in most bins. These results suggest that we can use the RRM as a ~~testbed~~ to address issues of intensity statistics over CONUS in the HR configurations of future EAM versions.

3.3.3 Diurnal cycle of summertime precipitation

Representing the correct timing and location of these convection episodes is of critical importance for precipitation prediction and hydrologic research (IPCC, 2012). Doing so requires the ability to capture many different meteorological phenomena. For example, summertime mesoscale convective complexes (MCCs) or systems (MCSs) contribute a significant amount of the total precipitation and play an important role in extreme precipitation events over the central US (Maddox, 1980; Carbone et al., 2002; Ashley et al., 2003; Tuttle and Davis, 2006), while disorganized convection strongly influences precipitation over the southeastern US (Dai et al., 1999; Bacmeister et al., 2014; Rickenbach et al., 2015). The diurnal cycle of precipitation is one important measure of a model's ability to reproduce these phenomena. For example, Bacmeister et al. (2014) used the diurnal cycle of precipitation to diagnose deficiencies in capturing the observed phase of MCSs over the central US in CAM5 with both LR and HR configurations.

Figure 15 illustrates the mean diurnal phase and magnitude patterns of maximum precipitation in JJA from the NEXRAD data and the EAMv1 simulations. The mean diurnal maximum is determined from the first harmonic of the Fourier series constructed from the hourly precipitation time series in each grid box. The phase (local time) of the maximum is indicated by colours, while the magnitude the saturation of the colour. The NEXRAD data (Fig. 15a) shows the distinct nocturnal (19:00–04:00 LT) peak over the central US. This nocturnal peak has been attributed to the eastward propagation of MCSs originating at the front range of Rocky Mountains in the afternoon (Riley et al., 1987; Dai et al., 1999; Carbone et al., 2002; Jiang et al., 2006; Dirmeyer et al., 2012). Unfortunately, no model configuration is successful at capturing this night time maximum. The RRM and HRM diurnal phases are similar and show modest improvement over the LRM in the sense that they have weaker amplitudes (lighter colours in panels c and d than in panel b) of incorrect diurnal cycles. The similarity between RRM and HRM indicates that RRM simulations will be valuable for understanding and addressing this important model bias.

To evaluate the known eastward propagation feature of the convection in this area, we average the JJA precipitation over four sub-regions: mountains, high plains, middle plains, and low plains, outlined by solid square boxes on Fig. 15a. Figure

Deleted: tool

Field Code Changed

Field Code Changed

Field Code Changed

Field Code Changed

Field Code Changed

16 shows the mean composite diurnal cycle in these sub-regions. We first calculate simple mean diurnal cycle from the hourly time series for each grid box. The first and second diurnal harmonics of the mean diurnal cycle — obtained using Fast Fourier Transform — are retained and adjusted to local time to generate the composite diurnal cycle. The composite lines plotted in Fig. 16 are averages of the composite diurnal cycle on each grid box within the sub-regions. In the NEXRAD measurements (Fig. 16a), there is a clear propagating pattern: the maximum emerges over the mountains (black) in the afternoon at 15:00, moves eastward and intensifies across the Great Plains, and reaches the middle (blue) and the low (green) plains in the night at 20:00 and 00:00, respectively. The three EAMv1 simulations (Fig. 16b-d) do not reproduce the convection propagation and miss the nocturnal precipitation peak. Although the HRM and the RRM show better skill than the LRM from the mountains to the high plains, these convective events are not strong enough (smaller magnitudes compared to observations) to sustain propagation further east.

The late afternoon rainfall peak over the southeast US is associated with disorganized convection (Bacmeister et al., 2014), a different mechanism than that over the central US. The red dashed lines in Fig. 16 denote the results for the southeast US. The diurnal cycle over the southeast US is generally well-simulated by the LRM, HRM, and RRM (panels b-d), but the time of peak precipitation is a few hours early, consistent with the experience of other models (Dai et al., 1999; Stratton and Stirling, 2012; Bechtold et al., 2014). More physically based improvements are needed to find a solution to the summertime diurnal cycle issue for precipitation over the CONUS, and the RRM provides an efficient ~~testbed~~ for parameterization testing. Previous studies (e.g., Bechtold et al., 2004; Stratton and Stirling, 2012; Bechtold et al., 2014) provide possible solutions for this issue of simulating the diurnal cycle of convective precipitation over land by modifying convective trigger procedures, entrainment, and convective closures. Our recent study (Xie et al., 2019) shows substantial improvement in the precipitation diurnal cycle in the LRM by employing a new convective trigger with a dynamic constraint on the convection onset, and with the capability of detecting moist instability above the boundary layer. We will apply the RRM testbed to extend the new convective trigger to the HRM and report the results in a future paper. This bias in the diurnal cycle of convection is significantly improved in convection-permitting (horizontal grid spacing < 2-4 km) simulations (Prein et al., 2015). The E3SM project is making progress in developing its convection-permitting version (E3SMv4), for which the RRM testbed will be heavily relied on.

Field Code Changed

Deleted: tool

Field Code Changed

4 Nudging capability for RRM

Nudging is an effective technique to create quasi-deterministic model realizations of observations for a specific time period. There is increasing use of nudging in climate model development and evaluation of physical parameterizations (e.g., Jeuken et al., 1996; Ghan et al., 2001; Kooperman et al., 2012; Zhang et al., 2014). Since nudging simulations constrain the model states closer to observed meteorological conditions, they facilitate evaluation of modelled physics during specific meteorological episodes. Therefore, nudging can help advance process-level understanding of physical phenomena, and

ultimately improve physical parameterizations. This is similar to the hindcast approach (Phillips et al., 2004; Ma et al., 2015) that has been widely used for climate model evaluation. EAMv1 has a built-in nudging capability as part of its physics module. When running the nudged RRM, one has various choices available such as nudging variables, locations, and time scales. In this section, we will provide an example of the value of EAMv1 RRM nudging simulations.

The EAMv1 nudging capability in the physics module allows relaxation of model state variables (U, V, T, and specific humidity, or a subset thereof) towards analysis/reanalysis data. The nudging strength is determined by a fractional nudging coefficient between zero and one, which can be a spatial constant or a spatial variable specified by a Heaviside window function. Following previous findings by Zhang et al. (2014) and Ma et al. (2015), we opt to only nudge horizontal velocities for better cloud and aerosol properties with a 6-hour relaxation time scale (see Eq. 1 of Zhang et al. 2014). The nudging coefficient map is shown in Fig. 17. The corresponding nudging parameter settings are documented in Table 3. This non-US nudging setting creates a smooth transition from the strongest nudging (red) over coarser grid points to the weakest nudging (blue) over finer grid points. Running in this mode builds a pseudo-regional model framework in a global model. It gives the simulation more freedom over part of the HR region and reduces the nudging noise due to inconsistency between the model and analysis data over the free-running region for better evaluation of physics over this region.

As an example of the nudging results, we create the Hovmöller diagrams (Fig. 18) of hourly mean total precipitation, meridionally averaged over 35°N–45°N, 93°W–115°W (the magenta box in Fig. 17) during the period of the DOE Atmospheric Radiation Measurement (ARM) Facility’s Midlatitude Continental Convective Clouds Experiment (MC3E, April 22 – June 6, 2011) (Jensen et al., 2016). The main science goal of the MC3E campaign is to improve the understanding of midlatitude continental convective cloud systems and their interactions with environment (Xie et al., 2014). Many cloud and precipitation events are observed and clearly shown from the NEXRAD panel (Fig. 18a), such as convective events on April 25 and around May 23, and widespread stratiform rain on May 10. As expected, the AMIP simulation (Fig. 18b) struggles to capture the statistics of these high-frequency weather systems. The RRM nudging simulation (Fig. 18c) reproduces the timing and location of most events because nudging the horizontal velocities outside of the analysed area provides more realistic boundary conditions of the large-scale circulation in the free-running domain. There are still some deficiencies in the nudged simulation, for example the incorrect number and propagating speed of convective events, particularly after May 15. The nudged RRM has cleanly separated these remaining (model-deficiency based) problems from issues related to the large-scale circulation. This demonstrates that the nudged RRM is an effective ~~testbed~~ for isolating and fixing parameterization problems at resolutions we cannot afford to run globally.

Field Code Changed

Field Code Changed

Deleted: approach

5 Summary and discussion

We have presented an overview of the climatological results comparing initial atmosphere-only simulations from globally uniform low-resolution (LR, 1°), high-resolution (HR, 0.25°), and regionally refined model (RRM, 1° to 0.25°) over the contiguous US (CONUS) with the atmosphere model version 1 (EAMv1) using the Energy Exascale Earth System Model (E3SM). Our analysis has established that the RRM can generally mimic HRM climate behaviour over the finely resolved portion (CONUS) for both well-simulated larger-scale thermodynamics fields and less-satisfactory smaller-scale physical variables.

Similar to other models (Dai, 2006; Bacmeister et al., 2014), the EAMv1 HRM suffers from deficiencies in convection, clouds, and moist physics (Xie et al., 2018). To verify that the RRM is a suitable alternative framework to the HRM to address these deficiencies, we examine the seasonal mean geographic patterns of precipitation, vertically-integrated precipitable water, low-level circulation, and surface temperature for JJA and DJF. Given its key importance in the atmospheric hydrologic cycle, we conduct in-depth analysis on precipitation, including fractions of the large-scale precipitation and daily intensity functions, and the JJA diurnal cycle. Overall, the RRM is similar to the HRM for many finer scale features, and including reproducing longstanding climate model biases, such as lack of summertime nocturnal precipitation peaks and the warm bias in surface air temperature.

Poor scale awareness of EAMv1 physical parameterizations necessitates retuning the model when increasing resolution. Different from previous RRM work using primarily the LR model (LRM) parameters, we make use of both LRM and HRM parameters and illustrate the significant impact of HR vs. LR parameters on RRM performance due to poor scale awareness, particularly for variables that are closely related to sub-grid scale physical processes. The high sensitivity of EAMv1 to model resolution suggests the need to develop better scale-aware physical parameterizations or convection-permitting simulations in the future. This study demonstrates how RRM can be used as a useful testbed to evaluate potentially improved schemes across different spatial scales.

To help users better utilize the E3SM RRM capability, we provide detailed guidance on running the RRM in the nudging mode so that deficiencies in model physical parameterizations can be better isolated. By relaxing the horizontal velocities over coarser resolution grids to analysis data, we create more realistic boundary conditions to the free-running higher resolution area. Such a pseudo-regional model framework within a global model displays great advantages in capturing observed convective episodes over the AMIP configuration, and hence allows us to calibrate simulated physical processes against observations under different meteorological conditions. With more realistic large-scale circulation conditions, the nudged RRM can be used as a physics testbed for regional process-level studies and aid in the development of future HR EAM versions.

Deleted: many
Field Code Changed

Deleted: tool
Deleted: test

Code availability: The E3SM source code is available on GitHub: <https://github.com/E3SM-Project/E3SM>.

Author contributions. QT and SAK designed the experiments. QT and WL performed the simulations and analyzed the data. QT, SAK, and SX designed the scope and structure of the manuscript. QT prepared the manuscript with contributions from all co-authors.

Acknowledgements. This research was primarily supported as part of the Energy Exascale Earth System Model (E3SM) project and partially supported by the Climate Model Development and Validation activity, [Atmospheric System Research Program](#), and an earlier project entitled Climate Science for a Sustainable Energy Future, funded by the U.S. Department of Energy (DOE), Office of Science, Office of Biological and Environmental Research (BER) under the auspices of the U.S. DOE by Lawrence Livermore National Laboratory under contract DE-AC52-07NA27344. The Pacific Northwest National Laboratory is operated for DOE by the Battelle Memorial Institute under contract DE-A06-76RLO 1830. This paper has been authored by employees of Brookhaven Science Associates, LLC, under contract No. DE-SC0012704 with the U.S. DOE. The publisher by accepting the paper for publication acknowledges that the U.S. Government retains a non-exclusive, paid-up, irrevocable, world-wide license to publish or reproduce the published form of this paper, or allow others to do so, for U.S. Government purposes. This research used resources of the National Energy Research Scientific Computing Center, a DOE Office of Science User Facility supported by the Office of Science of the U.S. DOE under Contract No. DE-AC02-05CH11231. This research used data from the Atmospheric Radiation Measurement Climate Research Facility. The E3SM simulation data used in this study can be downloaded at http://portal.nersc.gov/project/acme/tang30/E3SMv1_RRM_CONUS/. The ERA-Interim reanalysis data can be obtained from <http://apps.ecmwf.int/>. ISCCP cloud amount data are available from <https://isccp.giss.nasa.gov/products/browsed2.html>. GPCP and GPCP1DD precipitation datasets can be obtained from <https://www.csl.noaa.gov/psd/data/gridded/data.gpcp.html> and <ftp://meso.gsfc.nasa.gov/pub/1dd-v1.2/>. NEXRAD data are available from <https://data.nodc.noaa.gov/cgi-bin/iso?id=gov.noaa.ncdc:C00345>. CERES-EBAF top-of-atmosphere cloud radiative effects data can be downloaded at <https://ceres.larc.nasa.gov/products.php?product=EBAF-TOA>. The satellite data for COSP are archived at <http://climserv.ipsl.polytechnique.fr/cfmp-obs/>. The authors thank Christopher Terai for providing the GPCP1DD data. The authors also thank J. J. Gourley and Zac Flamig of the National Severe Storms Laboratory for access to the archives of NEXRAD NMQ Q2/3 products used in this study. LLNL-JRNL-764721.

References

- Ashley, W. S., Mote, T. L., Dixon, P. G., Trotter, S. L., Powell, E. J., Durkee, J. D. and Grundstein, A. J.: Distribution of Mesoscale Convective Complex Rainfall in the United States, *Mon. Weather Rev.*, 131(12), 3003–3017, doi:10.1175/1520-0493(2003)131<3003:DOMCCR>2.0.CO;2, 2003.
- Bacmeister, J. T., Wehner, M. F., Neale, R. B., Gettelman, A., Hannay, C., Lauritzen, P. H., Caron, J. M. and Truesdale, J. E.: Exploratory High-Resolution Climate Simulations using the Community Atmosphere Model (CAM), *J. Clim.*, 27(9), 3073–3099, doi:10.1175/JCLI-D-13-00387.1, 2014.
- Bader, D. C., Collins, W., Jacob, R., Jones, P., Rasch, P., Taylor, M., Thornton, P. and Williams, D.: Accelerated Climate Modeling for Energy, [online] Available from: <https://e3sm.org/wp-content/uploads/2018/03/ACME-project-strategy-July-2014.pdf>, 2014.
- Bechtold, P., Chaboureau, J.-P., Beljaars, A., Betts, A. K., Köhler, M., Miller, M. and Redelsperger, J.-L.: The simulation of the diurnal cycle of convective precipitation over land in a global model, *Q. J. R. Meteorol. Soc.*, 130(604), 3119–3137, doi:10.1256/qj.03.103, 2004.

Formatted: Bibliography, Widow/Orphan control, Adjust space between Latin and Asian text, Adjust space between Asian text and numbers

Field Code Changed

- Bechtold, P., Semane, N., Lopez, P., Chaboureaud, J.-P., Beljaars, A. and Bormann, N.: Representing Equilibrium and Nonequilibrium Convection in Large-Scale Models, *J. Atmospheric Sci.*, 71(2), 734–753, doi:10.1175/JAS-D-13-0163.1, 2014.
- Berg, L. K., Riihimäki, L. D., Qian, Y., Yan, H. and Huang, M.: The Low-Level Jet over the Southern Great Plains Determined from Observations and Reanalyses and Its Impact on Moisture Transport, *J. Clim.*, 28(17), 6682–6706, doi:10.1175/JCLI-D-14-00719.1, 2015.
- Bodas-Salcedo, A., Webb, M. J., Bony, S., Chepfer, H., Dufresne, J.-L., Klein, S. A., Zhang, Y., Marchand, R., Haynes, J. M., Pincus, R. and John, V. O.: COSP: Satellite simulation software for model assessment, *Bull. Am. Meteorol. Soc.*, 92(8), 1023–1043, doi:10.1175/2011BAMS2856.1, 2011.
- Bogenschütz, P. A., Gettelman, A., Morrison, H., Larson, V. E., Craig, C. and Schanen, D. P.: Higher-Order Turbulence Closure and Its Impact on Climate Simulations in the Community Atmosphere Model, *J. Clim.*, 26(23), 9655–9676, doi:10.1175/JCLI-D-13-00075.1, 2013.
- Carbone, R. E., Tuttle, J. D., Ahijevych, D. A. and Trier, S. B.: Inferences of Predictability Associated with Warm Season Precipitation Episodes, *J. Atmospheric Sci.*, 59(13), 2033–2056, doi:10.1175/1520-0469(2002)059<2033:IOPAWW>2.0.CO;2, 2002.
- Chepfer, H., Bony, S., Winker, D., Cesana, G., Dufresne, J. L., Minnis, P., Stubenrauch, C. J. and Zeng, S.: The GCM-Oriented CALIPSO Cloud Product (CALIPSO-GOCCP), *J. Geophys. Res.*, 115, doi:10.1029/2009JD012251, 2010.
- Cheruy, F., Dufresne, J. L., Hourdin, F. and Ducharme, A.: Role of clouds and land-atmosphere coupling in midlatitude continental summer warm biases and climate change amplification in CMIP5 simulations, *Geophys. Res. Lett.*, 41(18), 6493–6500, doi:10.1002/2014GL061145, 2014.
- Dai, A.: Precipitation Characteristics in Eighteen Coupled Climate Models, *J. Clim.*, 19(18), 4605–4630, doi:10.1175/JCLI3884.1, 2006.
- Dai, A., Giorgi, F. and Trenberth, K. E.: Observed and model-simulated diurnal cycles of precipitation over the contiguous United States, *J. Geophys. Res. Atmospheres*, 104(D6), 6377–6402, doi:10.1029/98JD02720, 1999.
- Dee, D. P., Uppala, S. M., Simmons, A. J., Berrisford, P., Poli, Kobayashi, S., Andrae, U., Balmaseda, M. A., Balsamo, G., Bauer, P., Bechtold, P., Beljaars, A. C. M., van de Berg, L., Bidlot, J., Bormann, N., Delsol, C., Dragani, R., Fuentes, M., Geer, A. J., Haimberger, L., Healy, S. B., Hersbach, H., Hólm, E. V., Isaksen, L., Kållberg, P., Köhler, M., Matricardi, M., McNally, A. P., Monge-Sanz, B. M., Morcrette, J. -J., Park, B. -K., Peubey, C., de Rosnay, P., Tavolato, C., Thépaut, J. -N. and Vitart, F.: The ERA-Interim reanalysis: configuration and performance of the data assimilation system, *Q. J. R. Meteorol. Soc.*, 137(656), 553–597, doi:10.1002/qj.828, 2011.
- Dennis, J. M., Edwards, J., Evans, K. J., Guba, O., Lauritzen, P. H., Mirin, A. A., St-Cyr, A., Taylor, M. A. and Worley, P. H.: CAM-SE: A scalable spectral element dynamical core for the Community Atmosphere Model, *Int. J. High Perform. Comput. Appl.*, 26(1), 74–89, doi:10.1177/1094342011428142, 2012.

- Dirmeyer, P. A., Cash, B. A., Kinter, J. L., Jung, T., Marx, L., Satoh, M., Stan, C., Tomita, H., Towers, P., Wedi, N., Achuthavariar, D., Adams, J. M., Altschuler, E. L., Huang, B., Jin, E. K. and Manganello, J.: Simulating the diurnal cycle of rainfall in global climate models: resolution versus parameterization, *Clim. Dyn.*, 39(1–2), 399–418, doi:10.1007/s00382-011-1127-9, 2012.
- 5 Fournier, A., Taylor, M. A. and Tribbia, J. J.: The Spectral Element Atmosphere Model (SEAM): High-Resolution Parallel Computation and Localized Resolution of Regional Dynamics, *Mon. Weather Rev.*, 132(3), 726–748, doi:10.1175/1520-0493(2004)132<0726:TSEAMS>2.0.CO;2, 2004.
- Gettelman, A. and Morrison, H.: Advanced Two-Moment Bulk Microphysics for Global Models. Part I: Off-Line Tests and Comparison with Other Schemes, *J. Clim.*, 28(3), 1268–1287, doi:10.1175/JCLI-D-14-00102.1, 2015.
- 10 Gettelman, A., Callaghan, P., Larson, V. E., Zarzycki, C. M., Bacmeister, J. T., Lauritzen, P. H., Bogenschutz, P. A. and Neale, R. B.: Regional Climate Simulations With the Community Earth System Model, *J. Adv. Model. Earth Syst.*, 10(6), 1245–1265, doi:10.1002/2017MS001227, 2018.
- Ghan, S., Laulainen, N., Easter, R., Wagener, R., Nemesure, S., Chapman, E., Zhang, Y. and Leung, R.: Evaluation of aerosol direct radiative forcing in MIRAGE, *J. Geophys. Res. Atmospheres*, 106(D6), 5295–5316, doi:10.1029/2000JD900502, 2001.
- 15 Giangrande, S. E., Collis, S., Theisen, A. K. and Tokay, A.: Precipitation Estimation from the ARM Distributed Radar Network during the MC3E Campaign, *J. Appl. Meteorol. Climatol.*, 53(9), 2130–2147, doi:10.1175/JAMC-D-13-0321.1, 2014.
- Gleckler, P., Doutriaux, C., Durack, P., Taylor, K. E., Zhang, Y., Williams, D., Mason, E. and Servonnat, J.: A more powerful reality test for climate models, *Eos Trans. Am. Geophys. Union*, 97, doi:10.1029/2016EO051663, 2016.
- 20 Golaz, J.-C., Larson, V. E. and Cotton, W. R.: A PDF-Based Model for Boundary Layer Clouds. Part I: Method and Model Description, *J. Atmospheric Sci.*, 59(24), 3540–3551, doi:10.1175/1520-0469(2002)059<3540:APBMFB>2.0.CO;2, 2002.
- Golaz, J.-C., Caldwell, P. M., Van Roekel, L. P., Petersen, M. R., Tang, Q., Wolfe, J. D., Abeshu, G., Anantharaj, V., Asay-Davis, X. S., Bader, D. C., Baldwin, S. A., Bisht, G., Bogenschutz, P. A., Branstetter, M., Brunke, M. A., Brus, S. R., Burrows, S. M., Cameron-Smith, P. J., Donahue, A. S., Deakin, M., Easter, R. C., Evans, K. J., Feng, Y., Flanner, M., Foucar, J. G., Fyke, J. G., Griffin, B. M., Hannay, C., Harrop, B. E., Hunke, E. C., Jacob, R. L., Jacobsen, D. W., Jeffery, N., Jones, P. W., Keen, N. D., Klein, S. A., Larson, V. E., Leung, L. R., Li, H.-Y., Lin, W., Lipscomb, W. H., Ma, P.-L., Mahajan, S., Maltrud, M. E., Mametjanov, A., McClean, J. L., McCoy, R. B., Neale, R. B., Price, S. F., Qian, Y., Rasch, P. J., Reeves Eyre, J. E. J., Riley, W. J., Ringler, T. D., Roberts, A. F., Roesler, E. L., Salinger, A. G., Shaheen, Z., Shi, X., Singh, B., Tang, J., Taylor, M. A., Thornton, P. E., Turner, A. K., Veneziani, M., Wan, H., Wang, H., Wang, S., Williams, D. N., Wolfram, P. J., Worley, P. H., Xie, S., Yang, Y., Yoon, J.-H., Zelinka, M. D., Zender, C. S., Zeng, X., Zhang, C., Zhang, K., Zhang, Y., Zheng, X., Zhou, T. and Zhu, Q.: The DOE E3SM coupled model version 1: Overview and evaluation at standard resolution, *J. Adv. Model. Earth Syst.*, 11, doi:10.1029/2018MS001603, 2019.
- 30

- Guba, O., Taylor, M. A., Ullrich, P. A., Overfelt, J. R. and Levy, M. N.: The spectral element method (SEM) on variable-resolution grids: evaluating grid sensitivity and resolution-aware numerical viscosity, *Geosci. Model Dev.*, 7(6), 2803–2816, doi:<https://doi.org/10.5194/gmd-7-2803-2014>, 2014.
- Helfand, H. M. and Schubert, S. D.: Climatology of the Simulated Great Plains Low-Level Jet and Its Contribution to the Continental Moisture Budget of the United States, *J. Clim.*, 8(4), 784–806, doi:[10.1175/1520-0442\(1995\)008<0784:COTSGP>2.0.CO;2](https://doi.org/10.1175/1520-0442(1995)008<0784:COTSGP>2.0.CO;2), 1995.
- Higgins, R. W., Yao, Y., Yarosh, E. S., Janowiak, J. E. and Mo, K. C.: Influence of the Great Plains Low-Level Jet on Summertime Precipitation and Moisture Transport over the Central United States, *J. Clim.*, 10(3), 481–507, doi:[10.1175/1520-0442\(1997\)010<0481:IOTGPL>2.0.CO;2](https://doi.org/10.1175/1520-0442(1997)010<0481:IOTGPL>2.0.CO;2), 1997.
- Hsu, J. and Prather, M. J.: Stratospheric variability and tropospheric ozone, *J. Geophys. Res. Atmospheres*, 114(D6), doi:[10.1029/2008JD010942](https://doi.org/10.1029/2008JD010942), 2009.
- Huang, X. and Ullrich, P. A.: The Changing Character of Twenty-First-Century Precipitation over the Western United States in the Variable-Resolution CESM, *J. Clim.*, 30(18), 7555–7575, doi:[10.1175/JCLI-D-16-0673.1](https://doi.org/10.1175/JCLI-D-16-0673.1), 2017.
- Huffman, G. J., Adler, R. F., Morrissey, M. M., Bolvin, D. T., Curtis, S., Joyce, R., McGavock, B. and Susskind, J.: Global Precipitation at One-Degree Daily Resolution from Multisatellite Observations, *J. Hydrometeorol.*, 2(1), 36–50, doi:[10.1175/1525-7541\(2001\)002<0036:GPAODD>2.0.CO;2](https://doi.org/10.1175/1525-7541(2001)002<0036:GPAODD>2.0.CO;2), 2001.
- Huffman, G. J., Adler, R. F., Bolvin, D. T. and Gu, G.: Improving the global precipitation record: GPCP Version 2.1, *Geophys. Res. Lett.*, 36(17), doi:[10.1029/2009GL040000](https://doi.org/10.1029/2009GL040000), 2009.
- IPCC: Managing the Risks of Extreme Events and Disasters to Advance Climate Change Adaptation, A Special Report of Working Groups I and II of the Intergovernmental Panel on Climate Change [Field, C.B., V. Barros, T.F. Stocker, D. Qin, D.J. Dokken, K.L. Ebi, M.D. Mastrandrea, K.J. Mach, G.-K. Plattner, S.K. Allen, M. Tignor, and P.M. Midgley (eds.)], Cambridge University Press, Cambridge, UK, and New York, NY, USA., 2012.
- Jensen, M. P., Petersen, W. A., Bansemer, A., Bharadwaj, N., Carey, L. D., Cecil, D. J., Collis, S. M., Del Genio, A. D., Dolan, B., Gerlach, J., Giangrande, S. E., Heymsfield, A., Heymsfield, G., Kollias, P., Lang, T. J., Nesbitt, S. W., Neumann, A., Poellot, M., Rutledge, S. A., Schwaller, M., Tokay, A., Williams, C. R., Wolff, D. B., Xie, S. and Zipser, E. J.: The Midlatitude Continental Convective Clouds Experiment (MC3E), *Bull. Am. Meteorol. Soc.*, 97(9), 1667–1686, doi:[10.1175/BAMS-D-14-00228.1](https://doi.org/10.1175/BAMS-D-14-00228.1), 2016.
- Jeuken, A. B. M., Siegmund, P. C., Heijboer, L. C., Feichter, J. and Bengtsson, L.: On the potential of assimilating meteorological analyses in a global climate model for the purpose of model validation, *J. Geophys. Res. Atmospheres*, 101(D12), 16939–16950, doi:[10.1029/96JD01218](https://doi.org/10.1029/96JD01218), 1996.
- Jiang, X., Lau, N. and Klein, S. A.: Role of eastward propagating convection systems in the diurnal cycle and seasonal mean of summertime rainfall over the U.S. Great Plains, *Geophys. Res. Lett.*, 33(19), doi:[10.1029/2006GL027022](https://doi.org/10.1029/2006GL027022), 2006.

- Klein, S. A., Jiang, X., Boyle, J., Malyshev, S. and Xie, S.: Diagnosis of the summertime warm and dry bias over the U.S. Southern Great Plains in the GFDL climate model using a weather forecasting approach, *Geophys. Res. Lett.*, 33(18), L18805, doi:10.1029/2006GL027567, 2006.
- 5 Klein, S. A., Zhang, Y., Zelinka, M. D., Pincus, R., Boyle, J. and Gleckler, P. J.: Are climate model simulations of clouds improving? An evaluation using the ISCCP simulator, *J. Geophys. Res. Atmospheres*, 118(3), 1329–1342, doi:10.1002/jgrd.50141, 2013.
- Kooperman, G. J., Pritchard, M. S., Ghan, S. J., Wang, M., Somerville, R. C. J. and Russell, L. M.: Constraining the influence of natural variability to improve estimates of global aerosol indirect effects in a nudged version of the Community Atmosphere Model 5, *J. Geophys. Res. Atmospheres*, 117(D23), doi:10.1029/2012JD018588, 2012.
- 10 Lin, Y., Zhao, M., Ming, Y., Golaz, J.-C., Donner, L. J., Klein, S. A., Ramaswamy, V. and Xie, S.: Precipitation Partitioning, Tropical Clouds, and Intraseasonal Variability in GFDL AM2, *J. Clim.*, 26(15), 5453–5466, doi:10.1175/JCLI-D-12-00442.1, 2013.
- Lin, Y., Dong, W., Zhang, M., Xie, Y., Xue, W., Huang, J. and Luo, Y.: Causes of model dry and warm bias over central U.S. and impact on climate projections, *Nat. Commun.*, 8(1), 881, doi:10.1038/s41467-017-01040-2, 2017.
- 15 Liu, X., Ma, P.-L., Wang, H., Tilmes, S., Singh, B., Easter, R. C., Ghan, S. J. and Rasch, P. J.: Description and evaluation of a new four-mode version of the Modal Aerosol Module (MAM4) within version 5.3 of the Community Atmosphere Model, *Geosci Model Dev.* 9(2), 505–522, doi:10.5194/gmd-9-505-2016, 2016.
- Loeb, N. G., Lyman, J. M., Johnson, G. C., Allan, R. P., Doelling, D. R., Wong, T., Soden, B. J. and Stephens, G. L.: Observed changes in top-of-the-atmosphere radiation and upper-ocean heating consistent within uncertainty, *Nat. Geosci.*, 5(2), 110–113, doi:10.1038/ngeo1375, 2012.
- 20 Ma, H.-Y., Klein, S. A., Xie, S., Zhang, C., Tang, S., Tang, Q., Morcrette, C. J., Van Weverberg, K., Petch, J., Ahlgrimm, M., Berg, L. K., Cheruy, F., Cole, J., Forbes, R., Gustafson, W. I., Huang, M., Liu, Y., Merryfield, W., Qian, Y., Roehrig, R. and Wang, Y. -C.: CAUSES: On the Role of Surface Energy Budget Errors to the Warm Surface Air Temperature Error Over the Central United States, *J. Geophys. Res. Atmospheres*, 123(5), 2888–2909, doi:10.1002/2017JD027194, 2018.
- 25 Ma, H.-Y., Xie, S., Klein, S. A., Williams, K. D., Boyle, J. S., Bony, S., Douville, H., Fermepin, S., Medeiros, B., Tyteca, S., Watanabe, M. and Williamson, D.: On the Correspondence between Mean Forecast Errors and Climate Errors in CMIP5 Models, *J. Clim.*, 27(4), 1781–1798, doi:10.1175/JCLI-D-13-00474.1, 2014.
- Ma, H.-Y., Chuang, C. C., Klein, S. A., Lo, M.-H., Zhang, Y., Xie, S., Zheng, X., Ma, P.-L., Zhang, Y. and Phillips, T. J.: An improved hindcast approach for evaluation and diagnosis of physical processes in global climate models, *J. Adv. Model. Earth Syst.*, 7(4), 1810–1827, doi:10.1002/2015MS000490, 2015.
- 30 Maddox, R. A.: Mesoscale Convective Complexes, *Bull. Am. Meteorol. Soc.*, 61(11), 1374–1387, doi:10.1175/1520-0477(1980)061<1374:MCC>2.0.CO;2, 1980.
- Mo, K. C. and Juang, H. H.: Relationships between soil moisture and summer precipitation over the Great Plains and the Southwest, *J. Geophys. Res. Atmospheres*, 108(D16), doi:10.1029/2002JD002952, 2003.

- Morcrette, C. J., Van Weverberg, K., Ma, H.-Y., Ahlgrim, M., Bazile, E., Berg, L. K., Cheng, A., Cheruy, F., Cole, J., Forbes, R., Gustafson, W. I., Huang, M., Lee, W.-S., Liu, Y., Mellul, L., Merryfield, W. J., Qian, Y., Roehrig, R., Wang, Y.-C., Xie, S., Xu, K.-M., Zhang, C., Klein, S. and Petch, J.: Introduction to CAUSES: Description of Weather and Climate Models and Their Near-Surface Temperature Errors in 5 day Hindcasts Near the Southern Great Plains, *J. Geophys. Res. Atmospheres*, 123(5), 2655–2683, doi:10.1002/2017JD027199, 2018.
- 5 Mueller, B. and Seneviratne, S. I.: Systematic land climate and evapotranspiration biases in CMIP5 simulations, *Geophys. Res. Lett.*, 1–7, doi:10.1002/2013GL058055, 2014.
- Neale, R. B., Chen, C. C., Gettelman, A., Lauritzen, P. H., Park, S., Williamson, D. L., Conley, A. J., Garcia, R., Kinnison, D., Lamarque, J. F., Marsh, D., Mills, M., Smith, A. K., Tilmes, S., Vitt, F., Cameron-Smith, P., Collins, W. D., Iacono, M. J., Easter, R. C., Ghan, S. J., Liu, X., Rasch, P. J. and Taylor, M. A.: Description of the NCAR Community Atmosphere Model (CAM5.0), Tech. Note NCAR/TN-486+STR, 274 pp., 2012.
- 10 NOAA: NOAA National Weather Service (NWS) Radar Operations Center (1991): NOAA Next Generation Radar (NEXRAD) Level 2 Base Data. NOAA National Centers for Environmental Information., doi:10.7289/V5W9574V, 2013.
- Pendergrass, A. G. and Hartmann, D. L.: Changes in the Distribution of Rain Frequency and Intensity in Response to Global Warming, *J. Clim.*, 27(22), 8372–8383, doi:10.1175/JCLI-D-14-00183.1, 2014.
- 15 Phillips, T. J., Potter, G. L., Williamson, D. L., Cederwall, R. T., Boyle, J. S., Fiorino, M., Hnilo, J. J., Olson, J. G., Xie, S. and Yio, J. J.: Evaluating Parameterizations in General Circulation Models: Climate Simulation Meets Weather Prediction, *Bull. Am. Meteorol. Soc.*, 85(12), 1903–1915, doi:10.1175/BAMS-85-12-1903, 2004.
- Pincus, R., Platnick, S., Ackerman, S. A., Hemler, R. S. and Patrick Hofmann, R. J.: Reconciling Simulated and Observed Views of Clouds: MODIS, ISCCP, and the Limits of Instrument Simulators, *J. Clim.*, 25(13), 4699–4720, doi:10.1175/JCLI-D-11-00267.1, 2012.
- 20 Prein, A. F., Langhans, W., Fosser, G., Ferrone, A., Ban, N., Goergen, K., Keller, M., Tölle, M., Gutjahr, O., Feser, F., Brisson, E., Kollet, S., Schmidli, J., Lipzig, N. P. M. van and Leung, R.: A review on regional convection-permitting climate modeling: Demonstrations, prospects, and challenges, *Rev. Geophys.*, 53(2), 323–361, doi:10.1002/2014RG000475, 2015.
- 25 Pu, B. and Dickinson, R. E.: Diurnal Spatial Variability of Great Plains Summer Precipitation Related to the Dynamics of the Low-Level Jet, *J. Atmospheric Sci.*, 71(5), 1807–1817, doi:10.1175/JAS-D-13-0243.1, 2014.
- Qian, Y., Jackson, C., Giorgi, F., Booth, B., Duan, Q., Forest, C., Higdon, D., Hou, Z. J. and Huerta, G.: Uncertainty Quantification in Climate Modeling and Projection, *Bull. Am. Meteorol. Soc.*, 97(5), 821–824, doi:10.1175/BAMS-D-15-00297.1, 2016.
- 30 Qian, Y., Wan, H., Yang, B., Golaz, J.-C., Harrop, B., Hou, Z., Larson, V. E., Leung, L. R., Lin, G., Lin, W., Ma, P.-L., Ma, H.-Y., Rasch, P., Singh, B., Wang, H., Xie, S. and Zhang, K.: Parametric Sensitivity and Uncertainty Quantification in the Version 1 of E3SM Atmosphere Model Based on Short Perturbed Parameter Ensemble Simulations, *J. Geophys. Res. Atmospheres*, 123(23), 13,046–13,073, doi:10.1029/2018JD028927, 2018.

- Rasch et al.: An Overview of the Atmospheric Component of the Energy Exascale Earth System Model, *J. Adv. Model. Earth Syst.*, submitted, 2019.
- Reynolds, R. W., Rayner, N. A., Smith, T. M., Stokes, D. C. and Wang, W.: An Improved In Situ and Satellite SST Analysis for Climate, *J. Clim.*, 15(13), 1609–1625, doi:10.1175/1520-0442(2002)015<1609:AIISAS>2.0.CO;2, 2002.
- 5 Rhoades, A. M., Huang, X., Ullrich, P. A. and Zarzycki, C. M.: Characterizing Sierra Nevada Snowpack Using Variable-Resolution CESM, *J. Appl. Meteorol. Climatol.*, 55(1), 173–196, doi:10.1175/JAMC-D-15-0156.1, 2016.
- Rickenbach, T. M., Nieto-Ferreira, R., Zarzar, C. and Nelson, B.: A seasonal and diurnal climatology of precipitation organization in the southeastern United States: Precipitation Organization in Southeastern USA, *Q. J. R. Meteorol. Soc.*, 141(690), 1938–1956, doi:10.1002/qj.2500, 2015.
- 10 Riley, G. T., Landin, M. G. and Bosart, L. F.: The Diurnal Variability of Precipitation across the Central Rockies and Adjacent Great Plains, *Mon. Weather Rev.*, 115(6), 1161–1172, doi:10.1175/1520-0493(1987)115<1161:TDVOPA>2.0.CO;2, 1987.
- Ringler, T., Ju, L. and Gunzburger, M.: A multiresolution method for climate system modeling: application of spherical centroidal Voronoi tessellations, *Ocean Dyn.*, 58(5–6), 475–498, doi:10.1007/s10236-008-0157-2, 2008.
- 15 Roesler et al.: Climatology of the Exascale Energy Earth System Model’s Atmospheric Model, version 0, Configured with Variable Resolution over the Continental United States, *Theor. Appl. Climatol.*, under review, 2018.
- Rossow, W. B. and Schiffer, R. A.: ISCCP Cloud Data Products, *Bull. Am. Meteorol. Soc.*, 72(1), 2–20, doi:10.1175/1520-0477(1991)072<0002:ICDP>2.0.CO;2, 1991.
- Seeley, J. T. and Roms, D. M.: The Effect of Global Warming on Severe Thunderstorms in the United States, *J. Clim.*, 28(6), 2443–2458, doi:10.1175/JCLI-D-14-00382.1, 2014.
- 20 Stephens, G. L., L’Ecuyer, T., Forbes, R., Gettelmen, A., Golaz, J.-C., Bodas-Salcedo, A., Suzuki, K., Gabriel, P. and Haynes, J.: Dreary state of precipitation in global models, *J. Geophys. Res. Atmospheres*, 115(D24), D24211, doi:10.1029/2010JD014532, 2010.
- Stratton, R. A. and Stirling, A. J.: Improving the diurnal cycle of convection in GCMs, *Q. J. R. Meteorol. Soc.*, 138(666), 1121–1134, doi:10.1002/qj.991, 2012.
- 25 Taylor, K. E.: Summarizing multiple aspects of model performance in a single diagram, *J. Geophys. Res. Atmospheres*, 106(D7), 7183–7192, doi:10.1029/2000JD900719, 2001.
- Taylor, M. A. and Fournier, A.: A compatible and conservative spectral element method on unstructured grids, *J. Comput. Phys.*, 229(17), 5879–5895, doi:10.1016/j.jcp.2010.04.008, 2010.
- 30 Terai, C. R., Caldwell, P. M., Klein, S. A., Tang, Q. and Branstetter, M. L.: The atmospheric hydrologic cycle in the ACME v0.3 model, *Clim. Dyn.*, 1–29, doi:10.1007/s00382-017-3803-x, 2017.
- Trenberth, K. E.: Changes in precipitation with climate change, *Clim. Res.*, 47(1–2), 123–138, doi:10.3354/cr00953, 2011.
- Tuttle, J. D. and Davis, C. A.: Corridors of Warm Season Precipitation in the Central United States, *Mon. Weather Rev.*, 134(9), 2297–2317, doi:10.1175/MWR3188.1, 2006.

- Van Weverberg, K., Morcrette, C. J., Petch, J., Klein, S. A., Ma, H. -Y., Zhang, C., Xie, S., Tang, Q., Gustafson, W. I., Qian, Y., Berg, L. K., Liu, Y., Huang, M., Ahlgrimm, M., Forbes, R., Bazile, E., Roehrig, R., Cole, J., Merryfield, W., Lee, W. -S., Cheruy, F., Mellul, L., Wang, Y. -C., Johnson, K. and Thieman, M. M.: CAUSES: Attribution of Surface Radiation Biases in NWP and Climate Models near the U.S. Southern Great Plains, *J. Geophys. Res. Atmospheres*, 123(7), 3612–3644, doi:10.1002/2017JD027188, 2018.
- Walsh, J., Wuebbles, D., Hayhoe, K., Kossin, J., Kunkel, K., Stephens, G., Thorne, P., Vose, R., Wehner, M., Willis, J., Anderson, D., Doney, S., Feely, R., Hennon, P., Kharin, V., Knutson, T., Landerer, F., Lenton, T., Kennedy, J. and Somerville, R.: Ch. 2: Our Changing Climate, in *Climate Change Impacts in the United States: The Third National Climate Assessment*, pp. 19–67. [online] Available from: doi:10.7930/J0KW5CXT (Accessed 24 April 2018), 2014.
- Williamson, D. L.: The effect of time steps and time-scales on parametrization suites, *Q. J. R. Meteorol. Soc.*, 139(671), 548–560, doi:10.1002/qj.1992, 2013.
- Wu, C., Liu, X., Lin, Z., Rhoades, A. M., Ullrich, P. A., Zarzycki, C. M., Lu, Z. and Rahimi-Esfarjani, S. R.: Exploring a Variable-Resolution Approach for Simulating Regional Climate in the Rocky Mountain Region Using the VR-CESM, *J. Geophys. Res. Atmospheres*, 122(20), 10,939-10,965, doi:10.1002/2017JD027008, 2017.
- Xie, S., Ma, H.-Y., Boyle, J. S., Klein, S. A. and Zhang, Y.: On the Correspondence between Short- and Long-Time-Scale Systematic Errors in CAM4/CAM5 for the Year of Tropical Convection, *J. Clim.*, 25(22), 7937–7955, doi:10.1175/JCLI-D-12-00134.1, 2012.
- Xie, S., Zhang, Y., Giangrande, S. E., Jensen, M. P., McCoy, R. and Zhang, M.: Interactions between cumulus convection and its environment as revealed by the MC3E sounding array, *J. Geophys. Res. Atmospheres*, 119(20), 2014JD022011, doi:10.1002/2014JD022011, 2014.
- Xie, S., Lin, W., Rasch, P. J., Ma, P.-L., Neale, R., Larson, V. E., Qian, Y., Bogenschutz, P. A., Caldwell, P., Cameron-Smith, P., Golaz, J.-C., Mahajan, S., Singh, B., Tang, Q., Wang, H., Yoon, J.-H., Zhang, K. and Zhang, Y.: Understanding Cloud and Convective Characteristics in Version 1 of the E3SM Atmosphere Model, *J. Adv. Model. Earth Syst.*, (10), doi:10.1029/2018MS001350, 2018.
- Xie, S., Wang, Y.-C., Lin, W., Ma, H.-Y., Tang, Q., Tang, S., Zheng, X., Golaz, J.-C., Zhang, G. and Zhang, M.: Diurnal Cycle of Precipitation Simulated by E3SM with a Revised Convective Trigger, *J. Adv. Model. Earth Syst.*, submitted, 2019.
- Yang, B., Qian, Y., Lin, G., Leung, L. R., Rasch, P. J., Zhang, G. J., McFarlane, S. A., Zhao, C., Zhang, Y., Wang, H., Wang, M. and Liu, X.: Uncertainty quantification and parameter tuning in the CAM5 Zhang-McFarlane convection scheme and impact of improved convection on the global circulation and climate, *J. Geophys. Res. Atmospheres*, 118(2), 395–415, doi:10.1029/2012JD018213, 2013.
- Zarzycki, C. M. and Jablonowski, C.: A multidecadal simulation of Atlantic tropical cyclones using a variable-resolution global atmospheric general circulation model, *J. Adv. Model. Earth Syst.*, 6(3), 805–828, doi:10.1002/2014MS000352, 2014.
- Zarzycki, C. M. and Jablonowski, C.: Experimental Tropical Cyclone Forecasts Using a Variable-Resolution Global Model, *Mon. Weather Rev.*, 143(10), 4012–4037, doi:10.1175/MWR-D-15-0159.1, 2015.

Zarzycki, C. M., Levy, M. N., Jablonowski, C., Overfelt, J. R., Taylor, M. A. and Ullrich, P. A.: Aquaplanet Experiments Using CAM's Variable-Resolution Dynamical Core, *J. Clim.*, 27(14), 5481–5503, doi:10.1175/JCLI-D-14-00004.1, 2014.

Zhang, J., Howard, K. and Gourley, J. J.: Constructing Three-Dimensional Multiple-Radar Reflectivity Mosaics: Examples of Convective Storms and Stratiform Rain Echoes, *J. Atmospheric Ocean. Technol.*, 22(1), 30–42, doi:10.1175/JTECH-1689.1, 2005.

Zhang, J., Howard, K., Langston, C., Vasiloff, S., Kaney, B., Arthur, A., Van Cooten, S., Kelleher, K., Kitzmiller, D., Ding, F., Seo, D.-J., Wells, E. and Dempsey, C.: National Mosaic and Multi-Sensor QPE (NMQ) System: Description, Results, and Future Plans, *Bull. Am. Meteorol. Soc.*, 92(10), 1321–1338, doi:10.1175/2011BAMS-D-11-00047.1, 2011.

Zhang, K., Wan, H., Liu, X., Ghan, S. J., Kooperman, G. J., Ma, P.-L., Rasch, P. J., Neubauer, D. and Lohmann, U.: Technical Note: On the use of nudging for aerosol–climate model intercomparison studies, *Atmospheric Chem. Phys.*, 14(16), 8631–8645, doi:https://doi.org/10.5194/acp-14-8631-2014, 2014.

Zhang, K., Rasch, P. J., Taylor, M. A., Wan, H., Leung, R., Ma, P.-L., Golaz, J.-C., Wolfe, J., Lin, W., Singh, B., Burrows, S., Yoon, J.-H., Wang, H., Qian, Y., Tang, Q., Caldwell, P. and Xie, S.: Impact of numerical choices on water conservation in the E3SM Atmosphere Model version 1 (EAMv1), *Geosci. Model Dev.*, 11(5), 1971–1988, doi:10.5194/gmd-11-1971-2018, 2018.

Zhang, Y., Xie, S., Covey, C., Lucas, D. D., Gleckler, P., Klein, S. A., Tannahill, J., Doutriaux, C. and Klein, R.: Regional assessment of the parameter-dependent performance of CAM4 in simulating tropical clouds, *Geophys. Res. Lett.*, 39(14), L14708, doi:10.1029/2012GL052184, 2012.

Zhang, Y., Xie, S., Lin, W., Klein, S. A., Zelinka, M., Ma, P.-L., Rasch, P. J., Qian, Y., Tang, Q. and Ma, H.-Y.: Evaluation of Clouds in Version 1 of the E3SM Atmosphere Model with Satellite Simulators, *J. Adv. Model. Earth Syst.*, 11, doi:10.1029/2018MS001562, 2019.

25

Deleted: Ashley, W. S., Mote, T. L., Dixon, P. G., Trotter, S. L., Powell, E. J., Durkee, J. D. and Grundstein, A. J.: Distribution of Mesoscale Convective Complex Rainfall in the United States, *Mon. Weather Rev.*, 131(12), 3003–3017, doi:10.1175/1520-0493(2003)131<3003:DOMCCR>2.0.CO;2, 2003.

Baumeister, J. T., Wehner, M. F., Neale, R. B., Gettelman, A., Hannay, C., Lauritzen, P. H., Caron, J. M. and Truesdale, J. E.: Exploratory High-Resolution Climate Simulations using the Community Atmosphere Model (CAM), *J. Clim.*, 27(9), 3073–3099, doi:10.1175/JCLI-D-13-00387.1, 2014.

Bader, D. C., Collins, W., Jacob, R., Jones, P., Rasch, P., Taylor, M., Thornton, P. and Williams, D.: Accelerated Climate Modeling for Energy, [online] Available from: <https://e3sm.org/wp-content/uploads/2018/03/ACME-project-strategy-July-2014.pdf>, 2014.

Berg, L. K., Riihimäki, L. D., Qian, Y., Yan, H. and Huang, M.: The Low-Level Jet over the Southern Great Plains Determined from Observations and Reanalyses and Its Impact on Moisture Transport, *J. Clim.*, 28(17), 6682–6706, doi:10.1175/JCLI-D-14-00719.1, 2015.

Bodas-Salcedo, A., Webb, M. J., Bony, S., Chepfer, H., Dufresne, J.-L., Klein, S. A., Zhang, Y., Marchand, R., Haynes, J. M., Pincus, R. and John, V. O.: COSP: Satellite simulation software for model assessment, *Bull. Am. Meteorol. Soc.*, 92(8), 1023–1043, doi:10.1175/2011BAMS2856.1, 2011.

Bogenschütz, P. A., Gettelman, A., Morrison, H., Larson, V. E., Craig, C. and Schanen, D. P.: Higher-Order Turbulence Closure and Its Impact on Climate Simulations in the Community Atmosphere Model, *J. Clim.*, 26(23), 9655–9676, doi:10.1175/JCLI-D-13-00075.1, 2013.

Carbone, R. E., Tuttle, J. D., Ahijevych, D. A. and Trier, S. B.: Inferences of Predictability Associated with Warm Season Precipitation Episodes, *J. Atmospheric Sci.*, 59(13), 2033–2056, doi:10.1175/1520-0469(2002)059<2033:IOPAWW>2.0.CO;2, 2002.

Chepfer, H., Bony, S., Winker, D., Cesana, G., Dufresne, J. L., Minnis, P., Stubenrauch, C. J. and Zeng, S.: The GCM-Oriented CALIPSO Cloud Product (CALIPSO-GOCCP), *J. Geophys. Res.*, 115, doi:10.1029/2009JD012251, 2010.

Cheruy, F., Dufresne, J. L., Hourdin, F. and Ducharme, A.: Role of clouds and land-atmosphere coupling in midlatitude continental summer warm biases and climate change amplification in CMIP5 simulations, *Geophys. Res. Lett.*, 41(18), 6493–6500, doi:10.1002/2014GL061145, 2014.

Dai, A.: Precipitation Characteristics in Eighteen Coupled Climate Models, *J. Clim.*, 19(18), 4605–4630, doi:10.1175/JCLI3884.1, 2006.

Dai, A., Giorgi, F. and Trenberth, K. E.: Observed and model-simulated diurnal cycles of precipitation over the contiguous United States, *J. Geophys. Res. Atmospheres*, 104(D6), 6377–6402, doi:10.1029/98JD02720, 1999.

Dee, D. P., Uppala, S. M., Simmons, A. J., Berrisford, P., Poli, Kobayashi, S., Andrae, U., Balmaseda, M. A., Balsamo, G., Bauer, P., Bechtold, P., Beljaars, A. C. M., van de Berg, L., Bidlot, J., Bormann, N., Delsol, C., Dragani, R., Fuentes, M., Geer, A. J., Haimberger, L., Healy, S. B., Hersbach, H., Hólm, E. V., Isaksen, I., Kållberg, P., Köhler, M., Matricardi, M., McNally, A. P., Monge-Sanz, B. M., Morcrette, J.-J., Park, B.-K., Peubey, C., de Rosnay, P., Tavolato, C., Thépaut, J.-N. and Vitart, F.: The ERA-Interim reanalysis: configuration and performance of the data assimilation system, *Q. J. R. Meteorol. Soc.*, 137(656), 553–597, doi:10.1002/qj.828, 2011.

Dennis, J. M., Edwards, J., Evans, K. J., Guba, O., Lauritzen, P. H., Mirin, A. A., St-Cyr, A., Taylor, M. A. and Worley, P. H.: CAM-SE: A scalable spectral element dynamical core for the Community

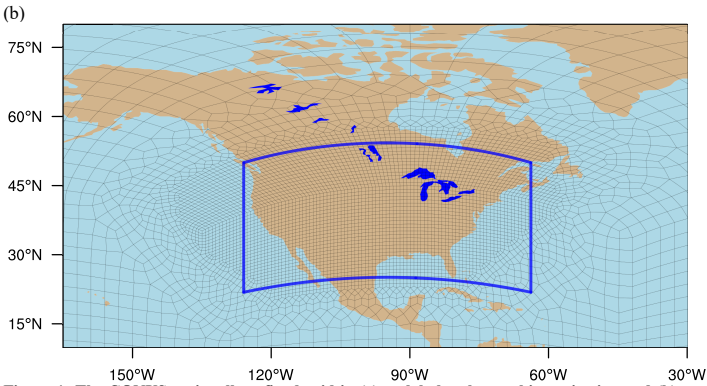
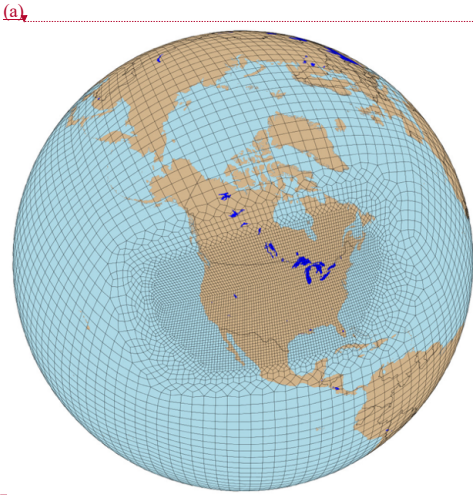


Figure 1: The CONUS regionally refined grid in (a) a global orthographic projection and (b) a cylindrical equidistant projection zoomed in over the high-resolution (HR) portion. The effective resolutions for the low-resolution (LR) and the HR regions are 1° and 0.25°, respectively. The two regions are connected with a transient area. The blue box (latitude range: 22°N–50°N, longitude range: 64°W–126°W) in panel (b) represents the analysed area for CONUS.

Deleted: ¶

Deleted: (a)

Formatted: Left, Line spacing: single

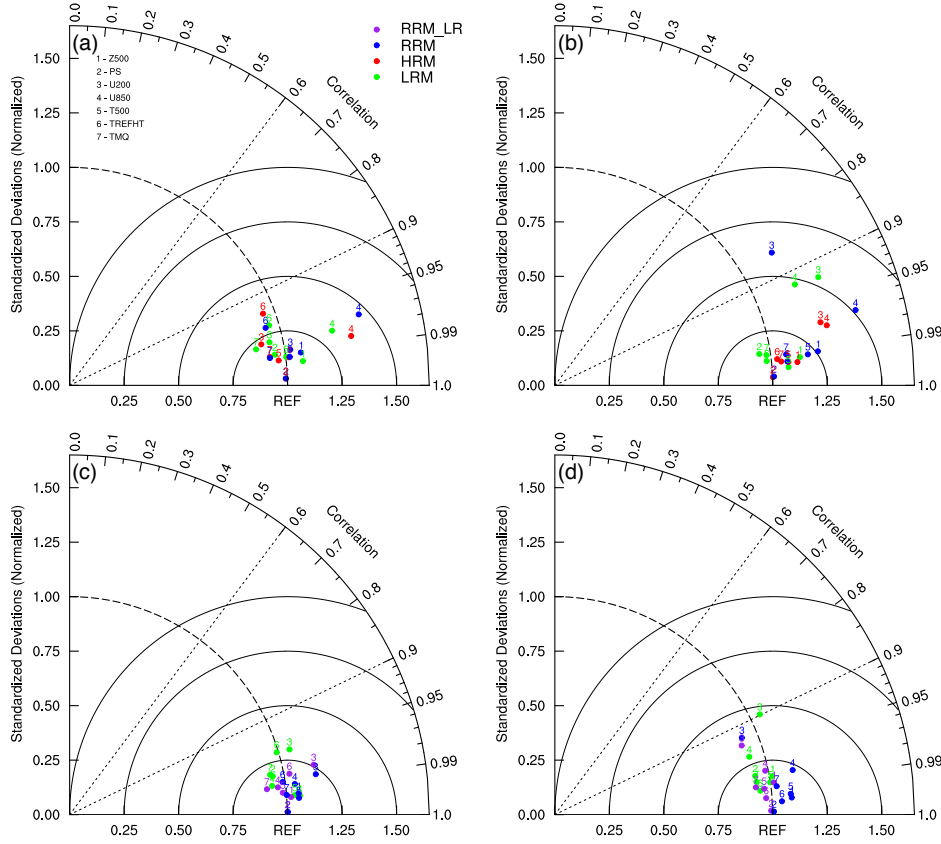


Figure 2: Taylor diagrams for three different model climatologies (color-coded: green – LRM, red – HRM, blue – RRM, and purple – RRM_LR) in JJA (left column) and DJF (right column). Results are from the CONUS domain (the blue box in Fig. 1b). For panels (a) and (b), verification data are used as the reference point (1, 0), and statistics are calculated on the coarser verification grids. For panels (c) and (d), the HRM is the reference, and statistics are calculated on the HRM grids. The numbers represent: 1 – 500-hPa geopotential height (Z500), 2 – surface pressure (PS), 3 – 200-hPa zonal wind (U200), 4 – 850-hPa zonal wind (U850), 5 – 500-hPa temperature (T500), 6 – 2-meter air temperature (TREFHT or T_{2m}), and 7 – total precipitable water (TMQ).

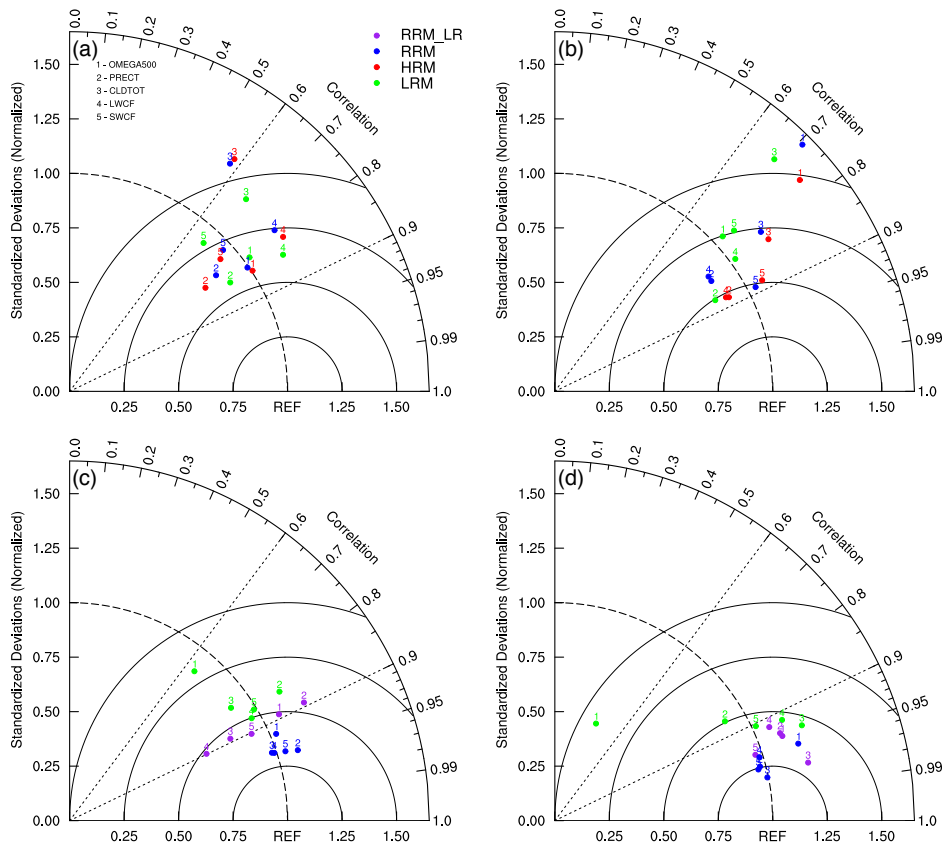


Figure 3: Same as Fig. 2, but the numbers represent: 1 – 500-hPa vertical velocity (OMEGA500), 2 – total precipitation (PRECT), 3 – vertically-integrated total cloud fraction (CLDTOT), 4 – longwave cloud forcing (LWCF), and 5 – shortwave cloud forcing (SWCF).

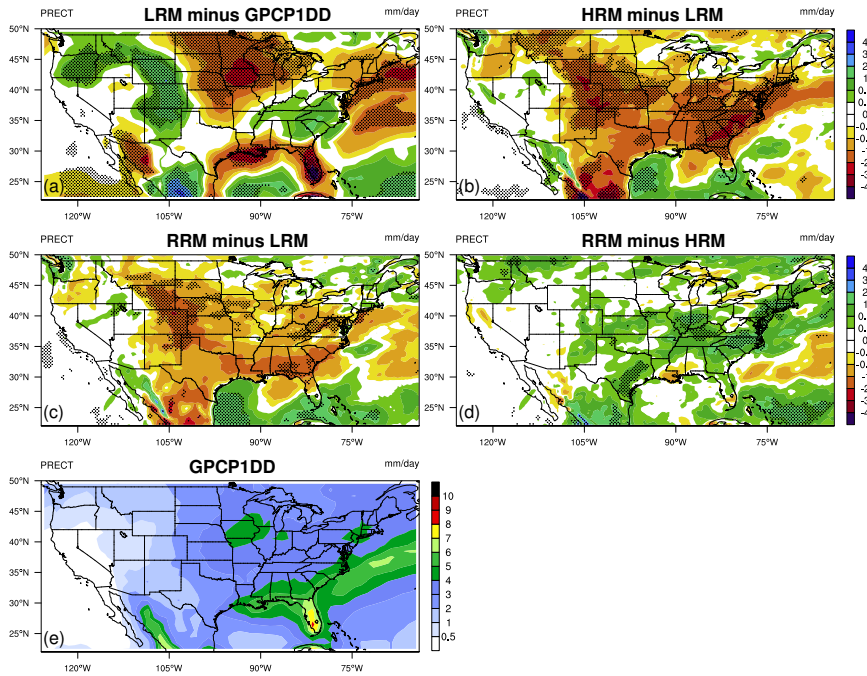
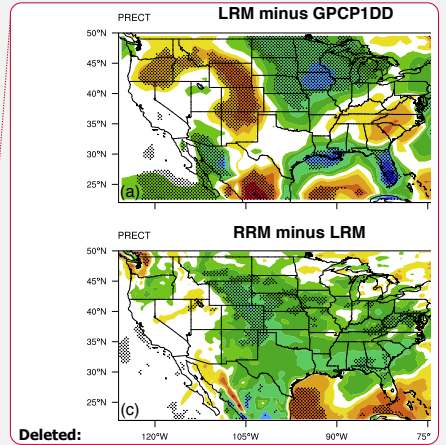


Figure 4: Mean differences of total precipitation (unit: mm/day) in JJA for (a) LRM minus GPCP1DD data, (b) HRM minus LRM, (c) RRM minus LRM, (d) RRM minus HRM, and (e) GPCP1DD. The differences between the LRM and evaluation data (i.e., panel a) are computed on the evaluation grid, while those between models (i.e., panels b-d) on the HRM grid. Dotted areas denote where the differences are statistically significant at the 95% confidence level with the two-tailed Student's *t*-test.



Deleted: and

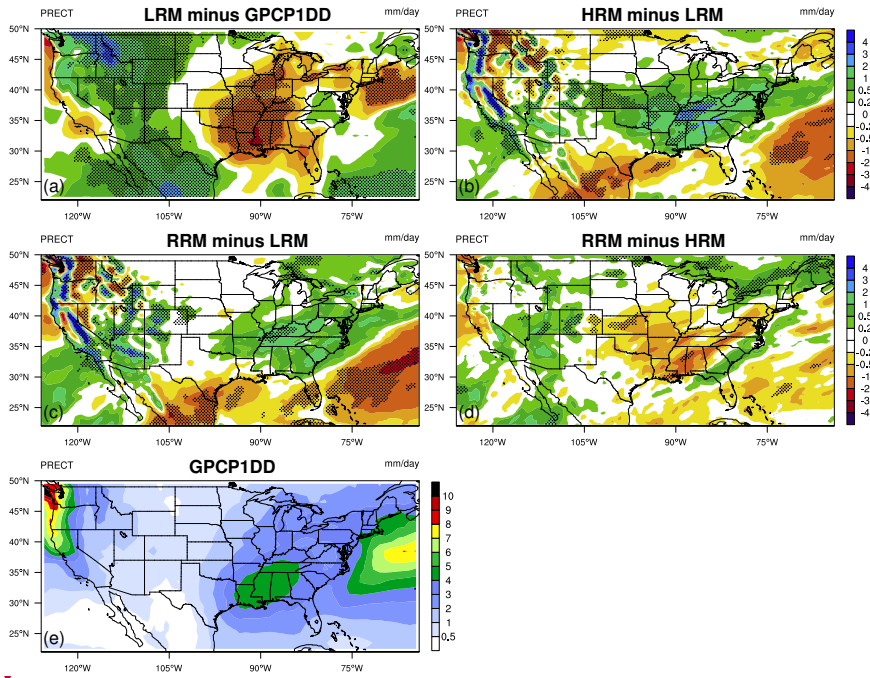
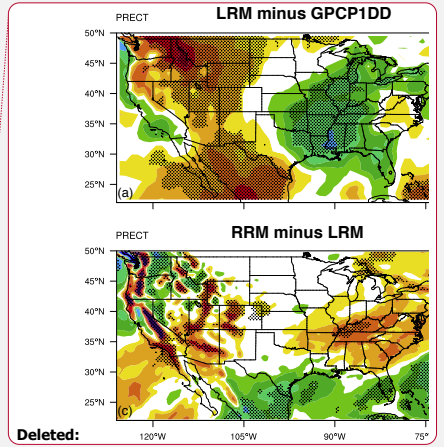


Figure 5: Same as Fig. 4, but for DJF.



Deleted:

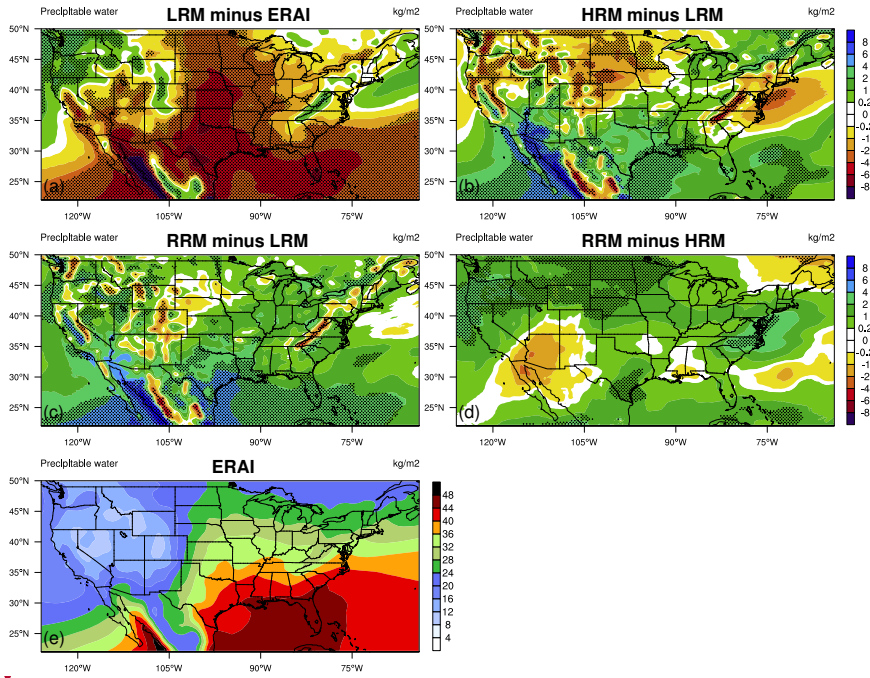
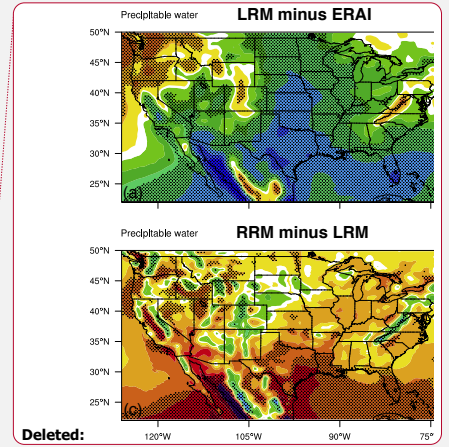


Figure 6: Same as Fig. 4, but for total precipitable water (TMQ, unit: kg/m^2) in JJA.



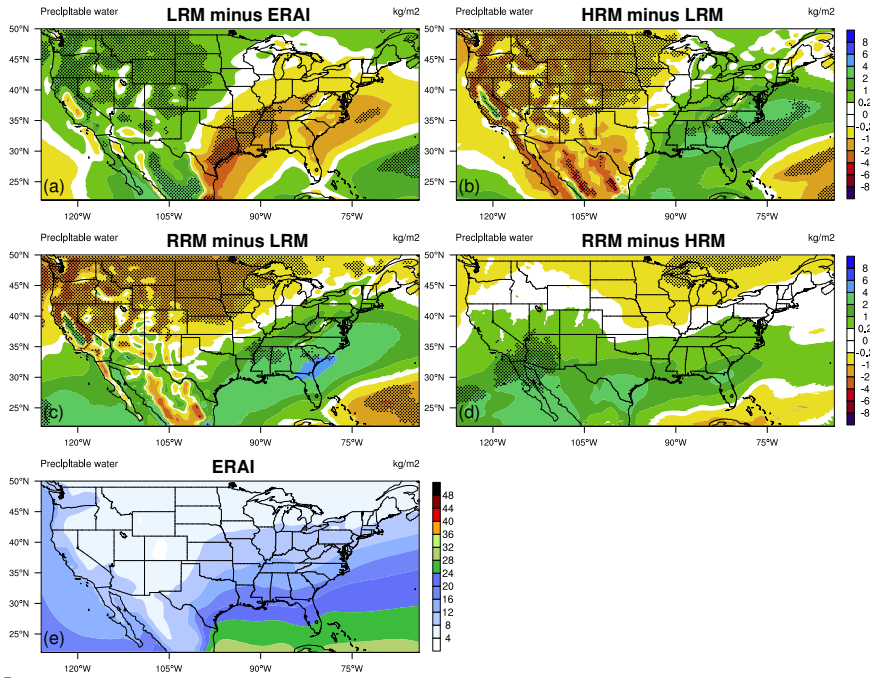
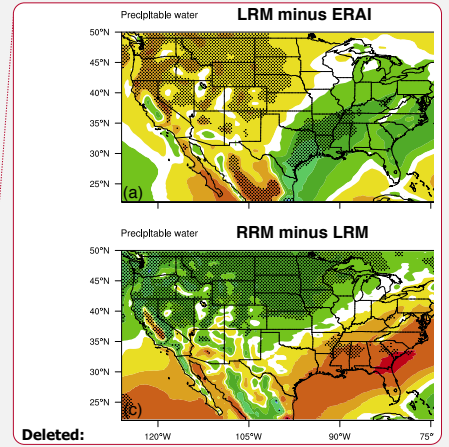


Figure 7: Same as Fig. 6, but for DJF.



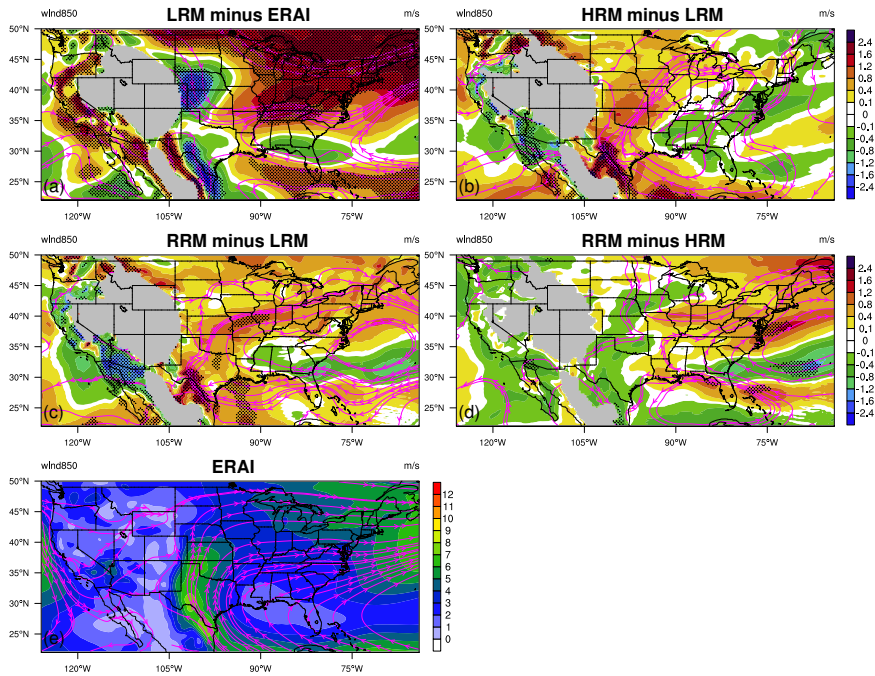
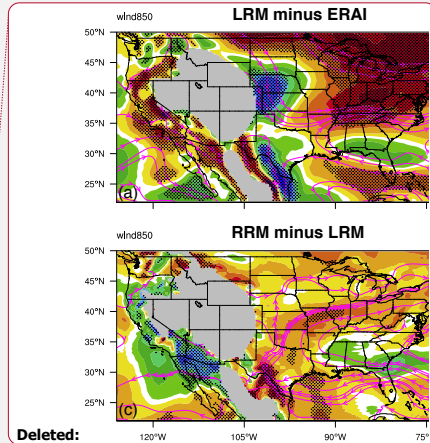


Figure 8: Same as Fig. 4, but for 850-hPa wind speed (unit: m/s) in JJA. The vectors are shown by colours (magnitudes) and magenta streamlines (directions). Grid boxes where surface pressure is less than 850 hPa are shaded in gray on the difference plots.



Deleted:

Deleted: difference

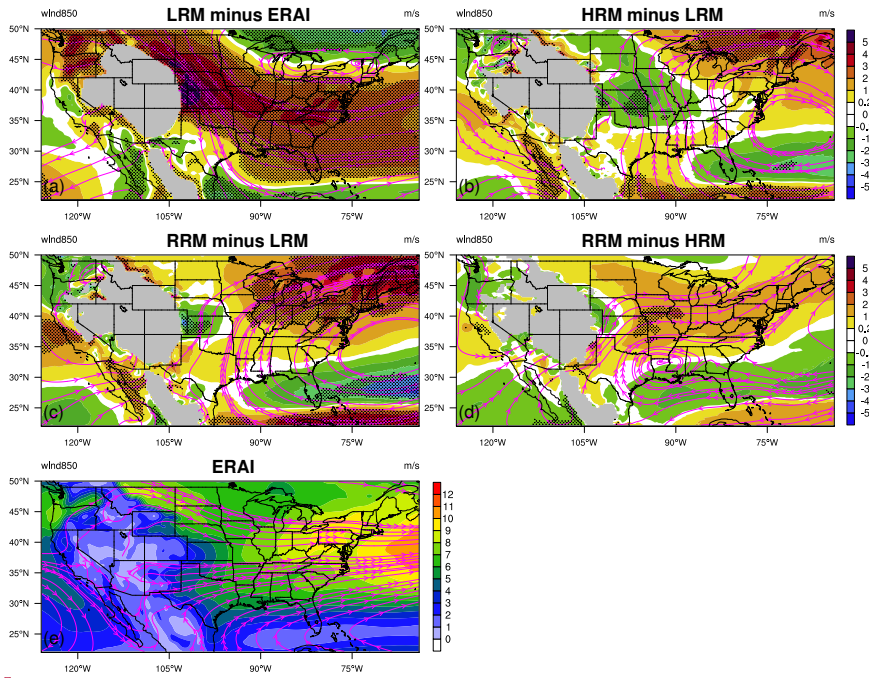
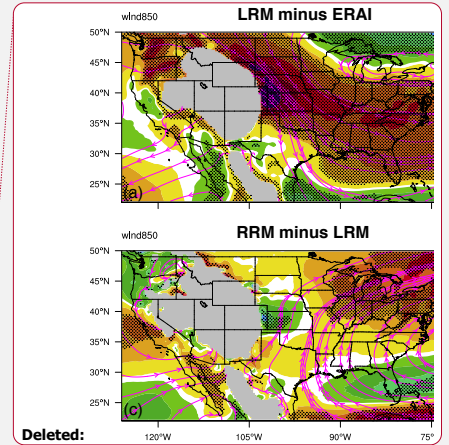


Figure 9: Same as Fig. 8, but for DJF. Note that the colour scale is different from that in Fig. 8.



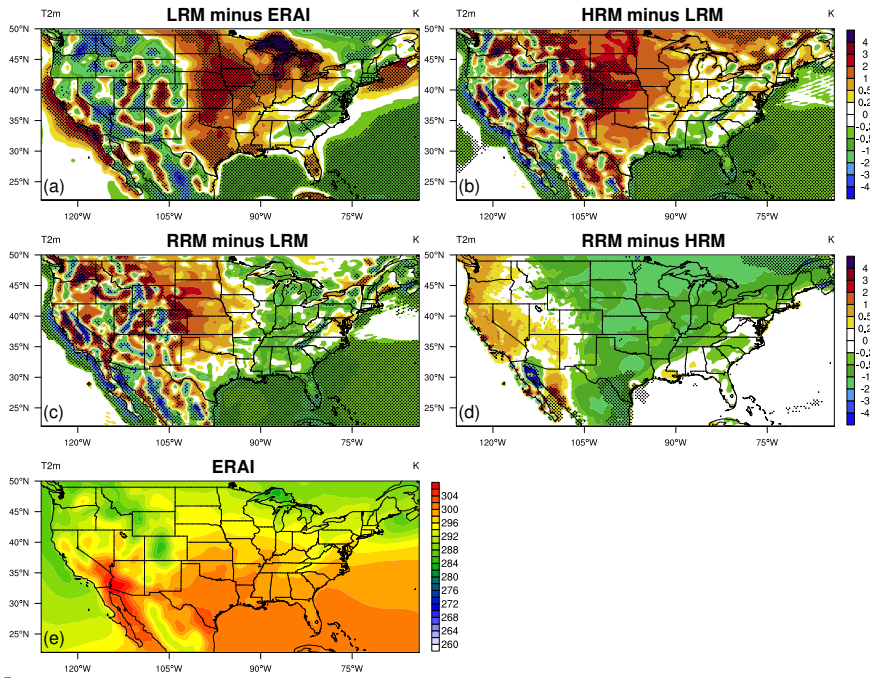
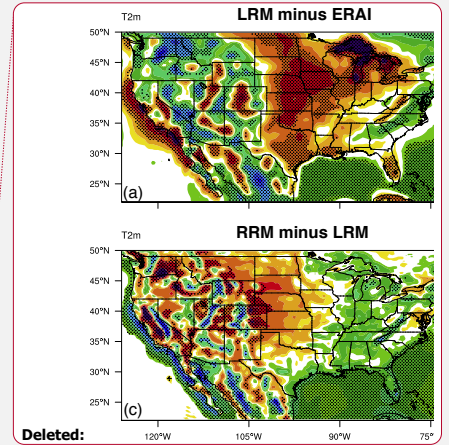


Figure 10: Same as Fig. 4, but for 2-meter air temperature (T_{2m} , unit: K) in JJA.



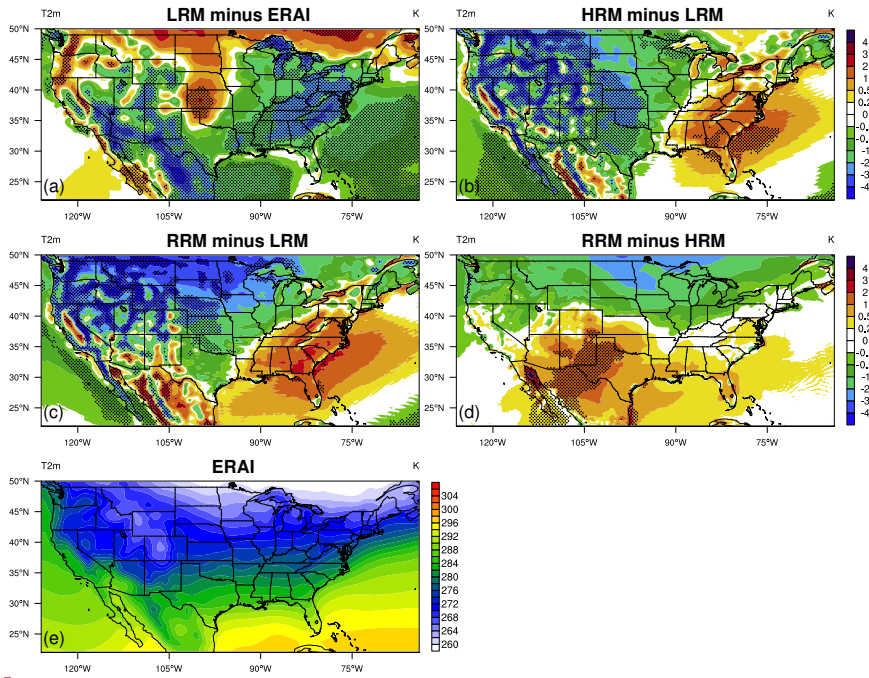


Figure 11: Same as Fig. 10, but for DJF.

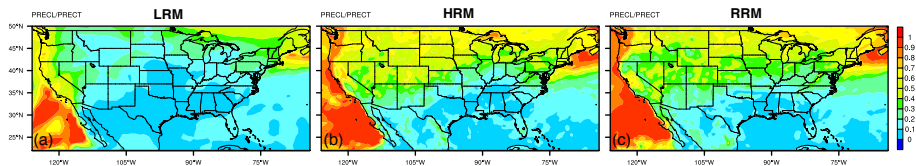
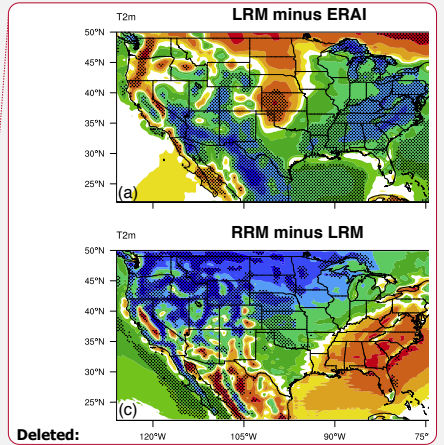


Figure 12: Mean ratio of large-scale to total precipitation in JJA for (a) LRM, (b) HRM, and (c) RRM.



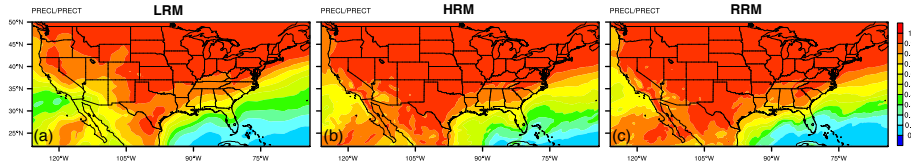
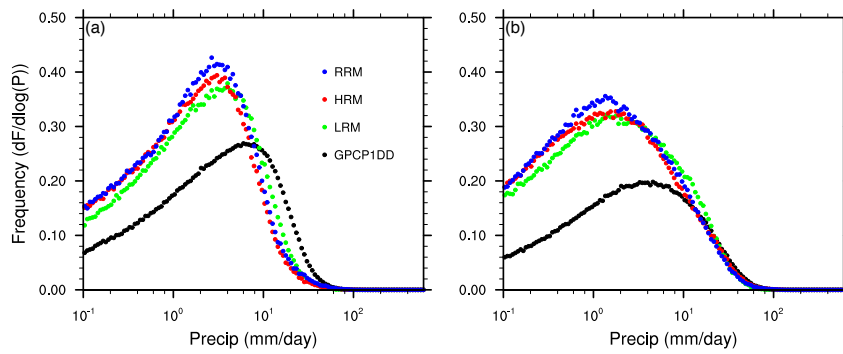


Figure 13: Same as Fig. 12, but for DJF.



5 Figure 14: Daily mean precipitation frequency (unit: $dF/d\log(P)$) functions of total precipitation for the GPCP1DD observation (black), and model simulations: LRM (green), HRM (red), and RRM (blue) in (a) JJA and (b) DJF. Before deriving the distribution, precipitation rates (unit: mm/day) are interpolated to $1^\circ \times 1^\circ$ grids and averaged over daily intervals.

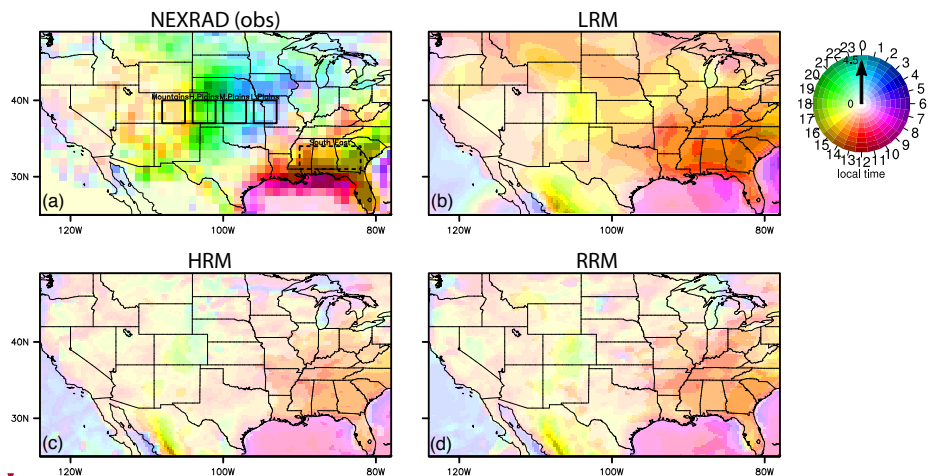
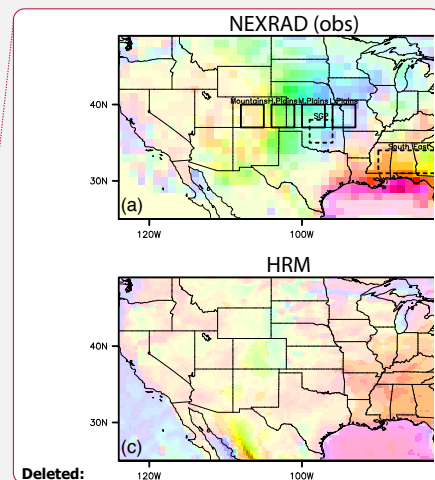


Figure 15: Mean diurnal phase (local time, unit: hours) and magnitude (unit: mm/day) of the maximum precipitation in JJA calculated from the first harmonic for (a) NEXRAD observations, (b) LRM, (c) HRM, and (d) RRM. The phase is indicated by colours, while the magnitude the saturation of the colour. In panel (a), the solid boxes denote 4 central US regions from west to east: mountains (37°N-40°N, 105°W-108°W), high plains (37°N-40°N, 101°W-104°W), middle plains (37°N-40°N, 97°W-100°W), and low plains (37°N-40°N, 93°W-96°W). The dashed box marks the southeast (31°N-34°N, 82°W-90°W) regions.



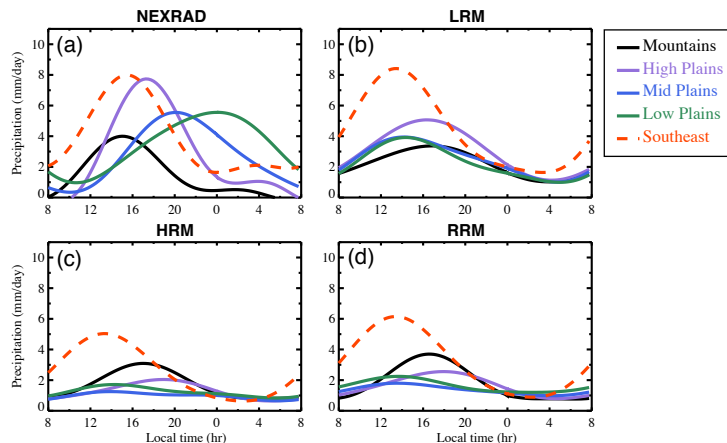


Figure 16: Mean JJA composite precipitation diurnal cycle from the NEXRAD and model simulations for the sub-regions (denoted in Fig. 15): mountains (black lines), high plains (purple lines), middle plains (blue lines), low plains (green lines), and southeast (red dashed lines). Panels represent for (a) NEXRAD, (b) LRM, (c) HRM, and (d) RRM. We first calculate simple mean diurnal cycle from the hourly time series for each grid box. The first and second diurnal harmonics of the mean diurnal cycle — obtained using Fast Fourier Transform — are retained and adjusted to local time to generate the composite diurnal cycle. The composite lines plotted here are averages of the composite diurnal cycle on each grid box within the sub-regions.

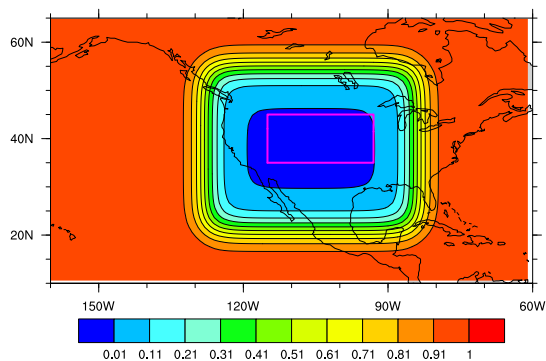


Figure 17: Nudging coefficient map zoom-in over North America. A coefficient of 0 represents that no nudging is applied. The magenta box marks the area of the Hovmöller plots in Fig. 18.

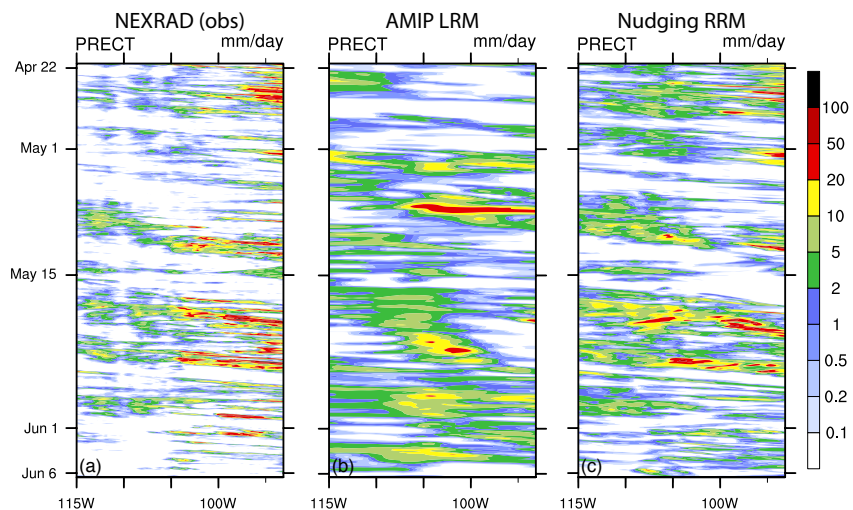


Figure 18: Hovmöller plots of hourly mean total precipitation (unit: mm/day) over 35°N–45°N, 93°W–115°W during April 22 – June 6, 2011 for (a) NEXRAD observations, (b) AMIP LRM, and (c) nudging RRM.

Table 1: **List of EAMv1 simulation configurations, speed, and costs. The speed and cost are for the NERSC Cori-KNL machine.**

Simulation	Configuration	Effective angular resolution	Number of elements	Speed (SYDP)	Number of nodes	Cost (core-hours/year)
Low-resolution model (LRM)	Default	1°	5400	6	81	22,000
High-resolution model (HRM)	Default	0.25°	86400	2	675	551,000
Regionally refined model (RRM)	HRM default	1° to 0.25°	9905	1.7	88	84,000
	RRM_LR	1° to 0.25°	9905	1.9	88	75,000
	LRM AMIP	1°	5400	6	81	22,000
RRM non-US nudging	HRM default	1° to 0.25°	9905	1.7	88	84,000

Table 2: **Summary list of observational and reanalysis-based evaluation datasets for model performance.**

Variable	Data source	Period	Reference	Web links
Z500, PS, U200, U850, T500 T _{2m} , TMQ, RH500, OMEGA500	ERA-Interim reanalysis	1989—2005	(Dee et al., 2011)	http://apps.ecmwf.int
CLDTOT	ISCCP	1983—2001	(Rossow and Schiffer, 1991)	https://isccp.giss.nasa.gov/products/browsed2.html
PRECT	GPCP	1979—2009	(Huffman et al., 2009)	https://www.esrl.noaa.gov/psd/data/gridded/data.gpcp.html
PRECT	GPCP1DD	1997—2013	(Huffman et al., 2001)	ftp://meso.gsfc.nasa.gov/pub/1dd-v1.2
PRECT	NEXRAD	2009—2013	(NOAA, 2013; Giangrande et al., 2014)	https://data.nodc.noaa.gov/cgi-bin/iso?id=gov.noaa.ncdc:C00345
LWCF, SWCF	CERES-EBAF	2000—2013	(Loeb et al., 2012)	https://ceres.larc.nasa.gov/products.php?product=EBAF-TOA
FISCCP1_COSP	ISCCP	1983—2008	(Pincus et al., 2012)	http://climserv.ipsl.polytechnique.fr/cfmip-obs
CLMODIS	MODIS	2002—2010	(Pincus et al., 2012; Zhang et al., 2012)	http://climserv.ipsl.polytechnique.fr/cfmip-obs
CLDTOT_CAL, CLDHGH_CAL, CLDMED_CAL, CLDLOW_CAL	CALIPSO	2006—2010	(Chepfer et al., 2010)	http://climserv.ipsl.polytechnique.fr/cfmip-obs

Deleted: List of
Deleted: s
Deleted: and the number of elements for each simulation
Formatted Table

Formatted Table

Formatted: Font: 9 pt
Formatted: Normal
Formatted: Font: 9 pt, Font color: Auto
Field Code Changed
Field Code Changed
Formatted: Font: 9 pt
Field Code Changed
Formatted: Font: 9 pt
Field Code Changed
Formatted: Font: 9 pt
Field Code Changed
Formatted: Font: 9 pt
Field Code Changed
Formatted: Font: 9 pt
Field Code Changed
Formatted: Font: 9 pt
Field Code Changed
Formatted: Font: 9 pt

Table 3: Nudging parameter settings for the non-US nudging simulation.

Nudging parameter	Value
Nudge_Model	.true.
Nudge_Path	Path to analysis/reanalysis data
Nudge_File_Template	'interim_se_%y%m%d00_%y%m%d18_TQUV- <u>%s</u> .nc'
Nudge_Times_Per_Day	4
Model_Times_Per_Day	96
Nudge_Uprof	2
Nudge_Ucoef	1.00
Nudge_Vprof	2
Nudge_Vcoef	1.00
Nudge_Tprof	0
Nudge_Tcoef	0.00
Nudge_Qprof	0
Nudge_Qcoef	0.00
Nudge_PSprof	0
Nudge_PSccoef	0.00
Nudge_Beg_Year	2011
Nudge_Beg_Month	1
Nudge_Beg_Day	1
Nudge_End_Year	2011
Nudge_End_Month	12
Nudge_End_Day	31
Nudge_Hwin_lo	1.0
Nudge_Hwin_hi	0.0
Nudge_Hwin_lat0	38.0
Nudge_Hwin_latWidth	34.0
Nudge_Hwin_latDelta	3.8
Nudge_Hwin_lon0	254.0
Nudge_Hwin_lonWidth	44.0
Nudge_Hwin_lonDelta	3.8
Nudge_Vwin_lo	0.0
Nudge_Vwin_hi	1.0
Nudge_Vwin_Hindex	73.0
Nudge_Vwin_Hdelta	0.1
Nudge_Vwin_Lindex	0.0
Nudge_Vwin_Ldelta	0.1

Formatted Table

Table 4: Acronym list.

ACME	Accelerated Climate Modeling for Energy
AMIP	Atmospheric Model Intercomparison Project
ARM	Atmospheric Radiation Measurement
CALIPSO	Cloud-Aerosol Lidar and Infrared Pathfinder Satellite Observation
CAM	Community Atmosphere Model
CERES-EBAF	Clouds and the Earth's Radiant Energy System—Energy Balanced and Filled
CESM	Community Earth System Model
CLUBB	Cloud Layers Unified By Binormals
CONUS	Contiguous United States
COSP	Cloud Feedback Model Intercomparison Project Observation Simulator Package
CSSEF	Climate Science for a Sustainable Energy Future
DJF	December-January-February
DOE	Department of Energy
E3SM	Energy Exascale Earth System Model
EAM	E3SM Atmosphere Model
EF	Evaporative Fraction
ENA	Eastern North Atlantic
ERA-I	European Centre for Medium-rang Weather Forecasting Interim
ESMF	Earth System Modeling Framework
GPCP	Global Precipitation Climatology Project
GPCP1DD	GPCP one-degree daily
HR	High-resolution
HRM	High-resolution Model
ISCCP	International Satellite Cloud Climatology Project
JJA	June-July-August
KNL	Knights Landing
Linoz	Linearized ozone chemistry
LLJ	Low-Level Jet
LR	Low-resolution
LRM	Low-resolution Model
MAM	Modal Aerosol Module
MCC	Mesoscale Convective Complex
MC3E	Midlatitude Continental Convective Clouds Experiment
MCS	Mesoscale Convective System
MODIS	Moderate Resolution Imaging Spectroradiometer
NERSC	National Energy Research Scientific Computing Center
NEXRAD	Next-Generation Radar
OMEGA500	500-hPa Vertical Velocity
PRECT	Total Precipitation
RMS	Root-Mean-Square
RRM	Regionally Refined Model
STD	Standard Deviation
SST	Sea Surface Temperature
TMQ	Total Precipitable Water
TREFHT	Reference Height Temperature

Formatted: Left

Formatted Table

Formatted Table

Formatted: Left

Formatted: Left

Formatted: Left

Formatted: Left

Formatted Table

Formatted: Left

Formatted: Left

Formatted Table

Formatted: Left

Formatted: Left

Formatted: Left

Formatted: Left

Formatted Table

Formatted: Left

Formatted Table

Formatted: Left

Formatted: Left

Formatted Table

Formatted Table

Formatted: Left

Formatted Table

<u>TWP</u>	<u>Tropical Western Pacific</u>
<u>U200</u>	<u>200-hPa Zonal Wind</u>
<u>US</u>	<u>United States</u>
<u>VR</u>	<u>Variable-resolution</u>

Formatted: Left

Formatted Table

Formatted: Left

Formatted Table

Appendix A

Table A1: EAMv1 simulation setup details. ^aUsed non-default parameter values in Table A2.

Simulation	Code hash	Grid	Compset
Low-resolution model (LRM)	7a17edbe5	ne30 ne30	FC5AV1C-04P2
High-resolution model (HRM)	66793a1d3	ne120 ne120	FC5AV1C-H01A
Regionally refined model (RRM)	7a17edbe5	conusx4v1 conusx4v1	FC5AV1C-04P2 ^a
RRM_LR	7a17edbe5	conusx4v1 conusx4v1	FC5AV1C-04P2
LRM AMIP	dd18fc56e	ne30 oECv3	F20TRC5-CMIP6
RRM non-US nudging	7a17edbe5	conusx4v1 conusx4v1	FC5AV1C-04P2 ^a

Table A2: Non-default parameter values.

Parameter	Value
cldfrc_dp1	0.03
clubb_c14	1.75
clubb_c8	4.73
rsplit	2
se_nsplit	6
cld_macmic_num_steps	3
zmconv_alfa	0.2
zmconv_c0_lnd	0.0035
zmconv_c0_ocn	0.0043
zmconv_dmpdz	-0.2e-3
zmconv_ke	5.0e-6

Formatted: Heading 1

Formatted: Superscript

Formatted Table

Formatted: Superscript

Formatted Table

Formatted: Centered

Formatted: Centered

Formatted: Centered

Formatted: Centered

Formatted: Centered

Formatted: Centered

Formatted Table

Formatted: Centered

✖